LA--9438-MS

DE83 003988

LA-9438-MS
(ISPO-172)
UC-15
Issued: October 1982

Nondestructive Verification with Minimal Movement of Irradiated Light-Water-Reactor Fuel Assemblies

J. R. Phillips
G. E. Bosler
J. K. Halbig
S. F. Klosterbuer
H. O. Menlove

Los Alamos National Laboratory
Los Alamos, New Mexico 87545

CONTENTS

FIGURES

TABLES

NONDESTRUCTIVE VERIFICATION WITH MINIMAL MOVEMENT OF IRRADIATED LIGHT-WATER REACTOR FUEL ASSEMBLIES

by

J. R. Phillips, G. E. Bosler, J. K. Halbig,
S. F. Klosterbuer, and H. O. Menlove

ABSTRACT

Nondestructive verification of irradiated light-water reactor fuel assemblies can be performed rapidly and precisely by measuring their gross gamma-ray and neutron signatures. A portable system measured fuel assemblies with exposures ranging from 18.4 to 40.6 GWd/tU and with cooling times ranging from 1575 to 2638 days. Differences in the measured results for side or corner measurements are discussed.

I. INTRODUCTION

Spent-fuel assemblies are accumulating at an increasingly rapid rate because of delays in nuclear fuel reprocessing. This potential source of very large and growing quantities of plutonium can have undesirable international consequences.[1] The primary objective of international safeguards is the

> timely detection of diversion of significant quantities of nuclear material from peaceful nuclear activities to the manufacture of nuclear weapons or of other nuclear explosive devices, or for purposes unknown, and deterrence of such diversion by the risk of early detection.[2]

The International Atomic Energy Agency (IAEA) is committed to the use of material accountancy as a fundamentally important technique for detection of a diversion, with containment and surveillance as important complementary measures.

The plutonium content of spent-fuel assemblies is of primary importance, with the residual ^{235}U content being less significant. The significant quantity (approximate quantity of special nuclear fissionable material required for a single explosive device) for plutonium has been generally accepted as 8 kg.[3] This amount is equivalent to the plutonium present in two pressurized-water reactor (PWR) or five boiling-water reactor (BWR) fuel assemblies discharged from typical facilities. Another important factor in evaluating the requirements for safeguarding spent-fuel assemblies is the time required to convert the plutonium present in the fuel assembly to a form compatible with the fabrication of a nuclear explosive. Time estimates for this conversion range from 1 to 3 months.[4] At present, the IAEA has established a detection time of a few months for irradiated materials with a desired detection probability of 95%.[5]

To verify the special nuclear material inventory of spent-fuel assemblies in a storage facility, a straightforward sampling plan could determine the number of fuel assemblies to be measured for the desired level of confidence. An approximate formula[6] for the detection probability provided by the attribute measurement of fuel assemblies is

$$DP = 1 - (1 - f)^D \quad , \tag{1}$$

where DP is the desired detection probability, f is the fraction of the total number of fuel assemblies that must be sampled, and D is the number of missing or altered fuel assemblies to be detected. To attain a 95% detection probability where D is 2 for PWR fuel assemblies and 5 for BWR fuel assemblies, the inspector would be required to select randomly and to measure approximately 80% of the PWR and 45% of the BWR fuel assemblies.

A variety of nondestructive measurement techniques is available for verifying spent-fuel assemblies, depending upon the level of verification required. Table I shows the relationship between the various gamma-ray and neutron measurement techniques and the specific levels of verification.[7] An inspector would not necessarily limit himself to either gamma-ray or neutron techniques but might combine the two techniques.

TABLE I

LEVELS OF VERIFICATION FOR SPENT-FUEL ASSEMBLIES

Specific Level of Verification	Nondestructive Technique		Instrumentation
	Gamma Ray	Neutron	
Physical characteristics			Visual inspection
Indication of irradiation exposure	Cerenkov		Cerenkov viewing device
	Presence of gamma radiation		Ion chambers Thermoluminescent detectors Scintillators
		Presence of neutron radiation	Fission chambers ^{10}B detectors
Physical integrity of fuel assembly	Cerenkov		Cerenkov viewing device
	Relative intensities of high-energy gamma rays		Germanium detectors Be(γ,n) detectors
		Relative values of neutron emission rates	Fission chambers ^{10}B detectors
Presence of fission products and actinides	Qualitative identification of specific gamma-ray lines		Germanium detectors Be(γ,n) detectors
		Relative values of neutron emission rates	Fission chambers ^{10}B detectors
Relative concentrations of fission products and actinides	Quantitative measurement of ^{137}Cs, $^{134}Cs/^{137}Cs$, and $^{154}Eu/^{137}Cs$. Correlation with operator-declared information		Germanium detectors
		Quantitative measurement of neutron emission rate. Correlation with operator-declared information	Fission chambers ^{10}B detectors
Direct measurement of special nuclear material	Indirectly through correlations between NDA measurements and destructive analyses		Germanium detectors
		Quantitative measurement of induced fissions in special nuclear material	Neutron source Fission chambers ^{10}B detectors

For reactors, the maximum time allocated for routine inspection is one-sixth of a man-year for each facility per calendar year.[2] An inspector cannot devote the entire inspection time to the verification of spent-fuel assemblies. He must review the auditing records and compare them with the IAEA reports, examine operating records and compare them with the accounting records, verify the fresh fuel assemblies before core loading, and verify the number of fuel assemblies in the reactor core following refueling and before closure of the reactor vessel.[4] Therefore, an inspector selects a level of verification consistent with the constraint of available time.

II. LEVELS OF VERIFICATION

A. Indication of Irradiation Exposure

The emission of gamma rays from a fuel assembly in the storage rack is a low-level verification. Two gamma-ray measurement techniques are available: (1) Cerenkov glow measurement[8,9] and (2) ion chamber or scintillator[10] measurements. The Cerenkov technique has the distinct advantage of performing the verification without placing any instrumentation into the storage pool water. But it has the disadvantage of requiring the elimination of most of the artificial lighting, forcing the inspector to move in a darkened environment, and increasing the safety hazard.

The gross gamma-ray signature of fuel assemblies also can be measured using ion chambers or scintillators or thermoluminescent detectors (TLDs). The signature is primarily from the activation products (^{60}Co, ^{58}Co, and ^{54}Mn) in the structural material at the top of the fuel assemblies, with the fission products (^{134}Cs, ^{137}Cs, and ^{144}Pr) also contributing. Ion chambers and scintillators provide the information immediately, whereas the TLDs must be removed from the water and subsequently read with a special instrument.

1. Cerenkov Glow Intensity Measurement.[8,9] Electromagnetic Cerenkov radiation is emitted whenever a charged particle passes through a medium with a velocity exceeding the phase velocity of light in that medium. In water, the phase velocity of light is about 75% of the value in vacuum. Any electron passing through water and having $\geq$0.26-MeV kinetic energy is thus a source of Cerenkov radiation. Irradiated fuel assemblies are prolific sources of beta

particles, gamma rays, and neutrons, all of which can produce Cerenkov light, directly or indirectly.

The normal fuel pin cladding (0.6- to 0.8-mm-thick Zircaloy) will absorb some of the beta particles originating in the fuel material; however, a significant fraction of the beta particles will enter the pool water and will be a significant source of Cerenkov light. It is possible that electron bremsstrahlung from energetic beta particles interacting in the fuel pins could be a significant source of gamma radiation in the pool water. In the cooling water, energetic fission product gamma rays can undergo pair production or Compton scattering to produce $\geq$0.26-MeV electrons. Neutrons may undergo H(n,γ) reactions in the water and produce Cerenkov light through interactions of the 2.23-MeV capture gamma rays with water.

The most significant production of Cerenkov light is from high-energy fission fragment-decay gamma rays that penetrate the cladding and fuel and interact with the water. The number of Cerenkov photons generated from gamma rays of any energy passing through water can be calculated. These calculations indicate that Cerenkov light production in the visible range of 4000-6000 Å is negligible for gamma rays with $E \leq 0.6$ MeV and rises steeply with greater gamma-ray energy. A gamma ray with E = 2 MeV produces more than 500 times the Cerenkov photons that are produced by a gamma ray with E = 0.6 MeV.

The information obtained from a Cerenkov measurement is related to burnup in that the absolute Cerenkov light level and its decay with time are related to burnup. If the Cerenkov light intensity is measured accurately, successful diversion either by substitution of dummy fuel assemblies or by incorrectly stating burnup should be difficult.

The spatial extent of the Cerenkov glow surrounding an isolated irradiated assembly in water probably is determined by the gamma radiation from the assembly's outer pins. The one-tenth-value-layer thickness of water for 1.0-MeV gamma rays is $\sim$36 cm, which is a reasonable estimate of the Cerenkov "halo" around an isolated point source. Fission product radiation from an irradiated fuel assembly's inner pins, however, must penetrate a much denser composite of fuel, cladding, and interstitial water that greatly reduces crosstalk among assemblies in either regular or high-density storage racks. The problem of crosstalk becomes significant when the gamma-ray field is measured above the fuel assemblies using ion chambers or scintillators (Sec. II.A.2).

The Cerenkov glow intensity measurement provides the inspector with a rapid nondestructive technique for verifying the presence of a gamma-ray source distributed within the fuel assembly. Where all the fuel pins can be seen, the image can be used to determine the removal of fuel pins from the fuel assembly. If several fuel pins were removed and were replaced with counterfeit fuel pins, an inspector might not detect the substitution. However, we stress that the intensity of the glow depends upon both the time since discharge from the reactor and the total exposure of the fuel assembly. The technique can provide a qualitative measurement for separating fuel assemblies into sets with similar gamma-ray source strengths without placing any equipment into the pool water.

2. Gross Gamma-Ray Measurements.[10,11] Ion chambers or scintillator detectors also can be used to verify the presence of gamma-ray radiation in spent-fuel assemblies in storage racks. Crosstalk between fuel assemblies located in adjacent storage positions must be reduced to a minimum to avoid the necessity of using unfolding techniques.[12] This measurement technique requires that the instrument

(1) be lightweight and easy to position by hand,

(2) give an immediate result,

(3) be undamaged by high-radiation levels, and

(4) ensure meaningful results.

Using a collimated germanium detector, we have measured the gamma-ray spectrum emitted from the top of two PWR fuel assemblies with exposures of 40.1 and 26.9 GWd/tU and cooling times of 1575 and 2049 days, respectively. The prominent gamma-ray lines in the spectrum were from the ^{60}Co, ^{137}Cs, and ^{134}Cs isotopes, with a very small contribution from the ^{144}Pr isotope. The long cooling times would have significantly reduced the contribution from ^{144}Pr, which is the daughter of the 285-day fission product ^{144}Ce. Cesium-137 and ^{134}Cs were dissolved in the pool water; therefore, it was not possible to determine quantitatively how much of the signals from these two isotopes was coming from the specific fuel assembly. The total signal coming from the fuel assembly was very low, as was the signal coming from the cesium dissolved in the pool water. The pool water was very clean, having much less cesium in it than would normally be expected at reactor spent-fuel storage pools. Cobalt-60 existed as a contaminant in the pool water as well as coming from the structural material of the fuel assemblies. Based upon our measurements, we cannot

confirm how much of the signals measured from the collimated germanium detector was due to the fission product inventory in the fuel assembly.

Ion chamber and scintillator detection techniques have been demonstrated to distinguish between fuel assemblies having widely differing exposures. They are rapid measurement techniques requiring only 1-2 min for positioning the detectors and collecting the data. For fuel assemblies stored in canisters, these are the only techniques for rapidly verifying the presence of radioactive material.

3. Neutron Measurements. Present technology does not permit the measurement of the neutron signals of spent-fuel assemblies by placing neutron detectors on top of the storage rack. The neutron flux, reduced by a factor of 10 for each 10 cm of water,[13] and the fuel material, located approximately 50 cm below the top of the storage racks, reduced the neutron source below the sensitivity level of most neutron detectors.

B. Physical Integrity of a Fuel Assembly

1. Cerenkov Glow Intensity Measurement. As discussed in Sec. II.A.1, this measurement technique has been used to determine the removal of individual fuel pins by examining the image and detecting anomalies in the glow pattern. For fuel assemblies with top plates, the fuel pins may not be visible; therefore, the technique is not fail safe.

2. Gross Gamma-Ray Measurements. Measurement of gross gamma-ray signals above fuel assemblies in a storage rack can detect only very large changes in the number of fuel pins present. However, removing the fuel assembly from the storage rack, that is, raising the assembly so measurements can be made from the side, significantly improves the detectability of fuel pin removal. In either measurement geometry, because of the source self-attenuation, the detectors only measure the gamma-ray signal from fuel pins located on the periphery of the fuel assembly.

The gamma-ray measurements can be improved by using a Be(γ,n) detector in which a ^{235}U fission chamber is surrounded by successive annuli of polyethylene and beryllium. Neutrons produced by a photoneutron reaction in the beryllium are thermalized in the polyethylene and then counted by the ^{235}U fission

chamber. Because the threshold for photoneutron production in beryllium is 1.66 MeV, the only significant fission product with a higher gamma-ray energy is the 2.186-MeV gamma ray of ^{144}Pr. The ^{144}Pr isotope, with a short half-life ($t_{1/2}$ = 17.3 min) is in secular equilibrium with its parent ^{144}Ce ($t_{1/2}$ = 284.5 days). Therefore, the Be(γ,n) detector measures the relative activity of ^{144}Ce.

The penetrability of the 2.186-MeV gamma ray is considerably greater than that of the majority of gamma rays from fission products ($\sim$0.6 MeV). Even the inner pins of a PWR fuel assembly can contribute to the 2.186-MeV source strength. For example, the fuel pins of the center row in the 15 x 15 fuel array can contribute 4% of the total flux of 2.186-MeV gamma rays at the surface of a fuel assembly, whereas for a 0.6-MeV gamma ray the self-attenuation has reduced its contribution to essentially 0.0. This measurement technique using a Be(γ,n) detector is not fail proof, but it is better than just measuring the gross gamma-ray signal with an ion chamber or scintillator to determine the absence of fuel pins.

C. Presence of Fission Products and Actinides

The presence of fission products can be detected only by using instrumentation that allows some type of energy resolution. The gamma-ray signatures of actinides cannot be measured directly because of the relatively high fission product background. A Be(γ,n) detector can be used to detect the presence of gamma rays with energies above 1.66 MeV and to infer the presence of the fission product ^{144}Pr. High-resolution gamma spectrometry (HRGS) using a germanium detector is the preferable technique for determining the presence of fission products. A spectrum obtained by HRGS can be used to qualitatively identify the source material by the comparison of the relative intensities of specific fission products. For example, the relative intensities of ^{106}Rh and ^{137}Cs can be used to identify qualitatively if the source material were ^{235}U or ^{239}Pu, because of the differences in the fission yields for ^{106}Ru-Rh (0.4% for ^{235}U and 4.3% for ^{239}Pu). Information about the time since discharge from the reactor also can be inferred by the presence or absence of fission products with short half-lives, for example, ^{95}Nb ($t_{1/2}$ = 34.97 days) and ^{95}Zr ($t_{1/2}$ = 63.98 days).

This level of verification ensures that fission products are present and that a dummy fuel pin has not been substituted. Without a confirmation of

fission products, an inspector cannot determine if the fuel pins have been replaced by ^{60}Co-activated pins. Therefore, this is a higher level of verification than other previously described techniques.

The presence of actinides can be inferred by the measurement of the neutron signature of the fuel assembly. Neutrons emitted from an irradiated fuel assembly can originate primarily from three sources:

(1) spontaneous fission of actinide isotopes;

(2) interaction of alpha particles from radioactive decay of transuranic isotopes (^{238}Pu, ^{241}Am, ^{242}Cm, and others) with ^{18}O in the oxide fuel; and

(3) induced fission in the fissile material from the first two sources.

Over short cooling times (less than a few weeks), photoneutron production from the 150 ppm of ^{2}H in natural water can be significant. Principal gamma rays with energies greater than the 2.2-MeV photoneutron reaction threshold come from the decay of ^{140}La ($t_{1/2}$ = 40.2 h), which is in equilibrium with its parent isotope ^{140}Ba ($t_{1/2}$ = 12.8 days). Another minor source of photoneutrons comes from a small number of high-energy gamma rays from ^{106}Rh ($t_{1/2}$ = 29.8 s), which is the daughter of ^{106}Ru ($t_{1/2}$ = 366.4 days). In this report, we assume that the number of neutrons originating from the photoneutron reactions is insignificant and that source neutrons originate primarily from the isotopes listed in Table II by the (α,n) reaction and spontaneous fission.

The curium isotopes are the dominant sources of neutrons within irradiated fuel assemblies with exposures above 10 GWd/tU (Ref. 14). As shown in Table II, most of the neutrons from ^{242}Cm and ^{244}Cm come from spontaneous fission, with $\bar{\nu}$ being 2.51 ± 0.06 for ^{242}Cm and 2.681 ± 0.011 for ^{244}Cm (Ref. 14). The plutonium isotopes can contribute a significant proportion to the total neutron source for fuel assemblies with relatively low exposures (<10 GWd/tU) or for fuel assemblies with extremely long cooling times (>100 yr). The uranium isotopes are significant neutron sources only in unirradiated fuel materials that do not contain transuranic isotopes.

The principal source of neutrons in a fuel assembly changes as the irradiation exposure increases. Figure 1 shows the calculated neutron production per cubic centimeter of fuel material for the five largest contributors to the total neutron signal. For the first case, an exposure of 10.9 GWd/tU, ^{242}Cm is the primary source at the time of discharge, with ^{244}Cm becoming the dominant source after 2 years of cooling. For higher exposures (>20 GWd/tU) the ^{244}Cm

TABLE II

PRINCIPAL SOURCES OF NEUTRONS IN IRRADIATED UO_2 MATERIALS

Isotope	Half-Life (yr)	(α,n)[a] Reaction	Spontaneous[a] Fission	Total[a]
^{235}U	7.04×10^{8}	7.11×10^{-4}	2.99×10^{-4}	1.01×10^{-3}
^{238}U	4.47×10^{9}	8.26×10^{-5}	1.36×10^{-2}	1.37×10^{-2}
^{238}Pu	8.78×10^{1}	1.34×10^{4}	2.59×10^{3}	1.60×10^{4}
^{239}Pu	2.41×10^{4}	3.81×10^{1}	2.18×10^{-2}	3.82×10^{1}
^{240}Pu	6.55×10^{3}	1.41×10^{2}	9.09×10^{2}	1.05×10^{3}
^{241}Pu	1.47×10^{1}	1.27×10^{0}	---[b]	1.27×10^{1}
^{242}Pu	3.76×10^{5}	2.05×10^{0}	1.72×10^{3}	1.71×10^{3}
^{241}Am	4.32×10^{2}	2.69×10^{3}	1.18×10^{0}	2.69×10^{3}
^{242}Cm	4.46×10^{-1}	3.76×10^{6}	2.10×10^{7}	2.48×10^{7}
^{244}Cm	1.81×10^{1}	7.73×10^{4}	1.08×10^{7}	1.09×10^{7}

[a]Neutrons per gram per second.

[b]Insignificant level.

is the dominant source of neutrons and is directly related to the fuel assembly exposure.[14]

D. Relative Concentrations of Fission Products and Actinides

1. Fission Products. For gamma-ray measurement techniques that are routinely applied to spent-fuel assemblies, HRGS is the most widely investigated and accepted technique.[7] The exposures of spent-fuel assemblies are generally correlated with ^{137}Cs, $^{134}Cs/^{137}Cs$, and $^{154}Eu/^{137}Cs$ in the HRGS methods. The ^{137}Cs isotope has a long half-life, similar fission yields for ^{235}U and ^{239}Pu, and an easily resolvable gamma-ray spectrum. Changes in the scanning geometry or the distribution of the source can affect the measured results. Using an isotopic ratio like $^{134}Cs/^{137}Cs$ or $^{154}Eu/^{137}Cs$, we can correct changes in the source attenuation with an internal relative efficiency calibration.[7,15] The initial ^{235}U enrichment can influence significantly the correlation of these two ratios with exposure. Therefore, some information about the initial enrichment is necessary for the correct interpretation of the results.

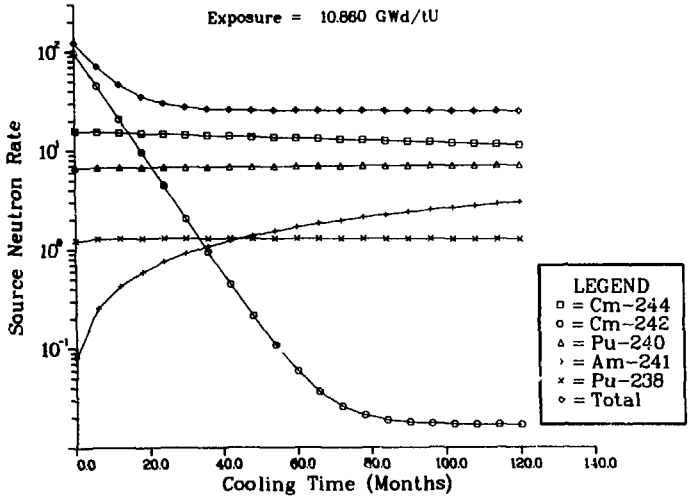

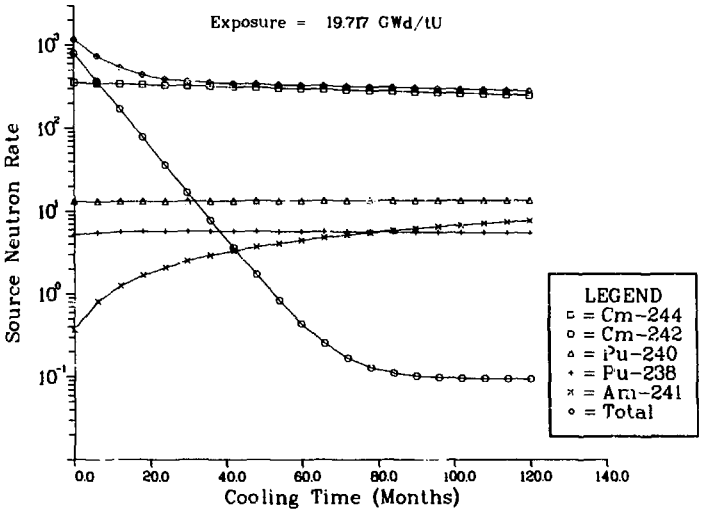

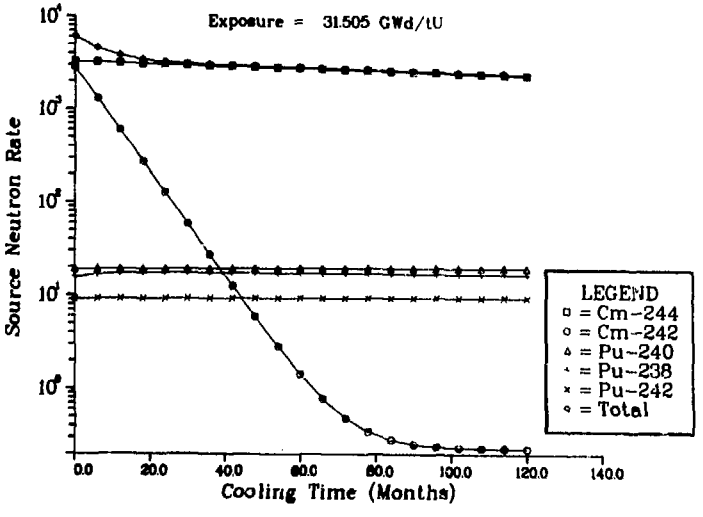

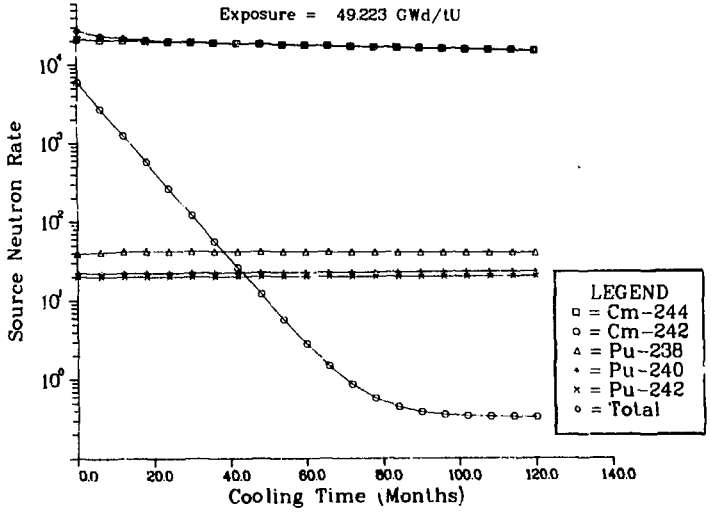

Fig. 1. Relative neutron source rates for each of the five largest contributors to the total neutron rate.

Some experimenters have attempted to establish correlations between the number of days since discharge and various isotopic concentrations and ratios.[16,17] Knowledge of the cooling time is of particular importance for the $^{134}Cs/^{137}Cs$ ratio because of the relatively short half-life of ^{134}Cs ($t_{1/2}$ = 2.062 yr). Cooling time is also important in the interpretation of the passive neutron measurements of spent-fuel assemblies. The primary sources of neutrons in irradiated fuel materials are ^{242}Cm ($t_{1/2}$ = 163 days) and ^{244}Cm ($t_{1/2}$ = 18.11 yr); if the cooling time is greater than 3 years, the source is only related to the build-up of ^{244}Cm for exposures above 10 GWd/tU.

Gamma-ray measurements should be interpreted cautiously. How much of the volume of the fuel assembly do they represent? For a PWR fuel assembly, only the outer three or four rows of fuel pins contribute to the ^{134}Cs and ^{137}Cs signals. Table III gives the percentage of the total gamma-ray signal derived from each row of fuel pins. These values were calculated using a Monte Carlo technique to track each photon originating in the specific fuel pin positions.

For verification, HRGS is currently the most widely accepted technique; however, the inspector must consider the source self-attenuation, as shown in Table III. This table illustrates the advantage of using a high-energy rather than a lower energy gamma ray to obtain a representative signature of the cross section of a fuel assembly. The measurement technique has been applied to BWR fuel assemblies and compared with destructive measurements with reasonably good success.[7]

TABLE III

PERCENTAGE OF GAMMA RAYS FROM EACH ROW
BASED ON THE TOTAL VALUE

Isotope	Energy (keV)	Row Number 1 (%)	2 (%)	3 (%)	4 (%)
^{134}Cs	605	67.6	20.6	8.6	3.2
^{134}Cs	796	54.0	22.4	11.9	5.2
^{137}Cs	662	61.5	20.7	9.5	3.5
^{154}Eu	1274	40.2	22.4	15.2	7.7
^{144}Pr	2186	32.8	20.7	15.9	9.1

2. Actinide Concentrations. The neutron source rate is related to the exposure of spent-fuel assemblies with exposures above 10 GWd/tU by a power functional relationship (Fig. 2). This relationship has been confirmed by calculational and experimental measurements.[14] The penetrability of neutrons is much greater than that of gamma rays; therefore, neutron measurement more accurately samples the entire cross section of the fuel assembly.

Instrumentation for measuring the neutron signature of fuel assemblies includes a neutron detector (probably a ^{235}U fission chamber), the power supply, an amplifier, and a scaler/timer. Relatively simple and easily operated, these instruments measure a single midpoint in less than 5 min per fuel assembly.

E. Direct Measurement of Special Nuclear Material

The neutron and gamma-ray signatures of uranium and plutonium isotopes cannot be measured directly because of interference from other actinides and fission products. As shown in Fig. 1, most of the neutrons came from the curium isotopes, with only a small percentage of neutrons originating in ^{240}Pu and ^{238}Pu.

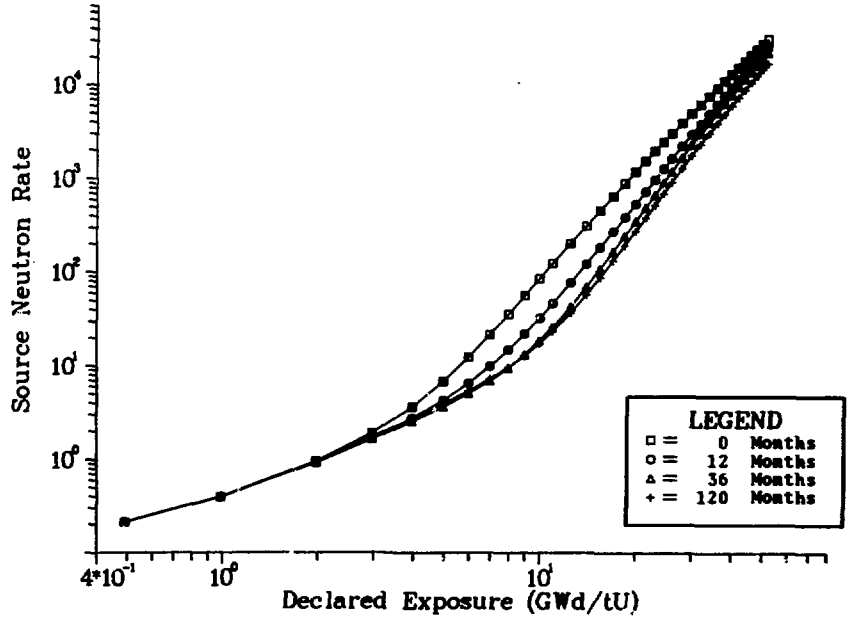

Fig. 2. Neutron source rate as a function of exposure for four cooling times.

Uranium-235 and ^{239}Pu gamma-ray lines cannot be measured using HRGS because of the large numbers of fission product gamma rays. For irradiated reactor fuel with 30 GWd/tU exposure, the prominent 414-keV line of ^{239}Pu has an intensity of only 1392 gamma rays/cm^3/s, whereas the fission product ^{137}Cs emits 4.38×10^{10} gamma rays/cm^3/s. For each ^{239}Pu 414-keV gamma ray emitted, more than 30 000 000 gamma rays are emitted from the single fission product ^{137}Cs. Any gamma ray from the fissile isotopes is completely overwhelmed by the fission product gamma rays and their associated Compton backgrounds. Therefore, the concentration of fissile isotopes in spent fuel must be measured indirectly by relating the build-up of specific fission products to the depletion of the ^{235}U and the build-up of plutonium.

III. EXPERIMENTAL MEASUREMENTS

Based on the above discussions of the measurement techniques available for each level of verification, we selected a combination of gamma-ray and neutron measurements as the most cost-effective and practical considering the quality of information collected and time required for the measurements. By determining the gross gamma-ray signatures of the fuel assemblies, an inspector can obtain a qualitative measurement of the consistency of the operator-declared cooling times. Figure 3 shows the relationship between the calculated response from PWR fuel assemblies divided by the exposure as a function of cooling time. The curve approximates a power function decay curve with the power factor being approximately equal to -1 with respect to cooling time. Having collected a set of measurements of the gross gamma-ray doses, an inspector can plot the data on a similar curve to determine the internal consistency of the measured data set.

The second measurement, performed simultaneously with the gamma-ray measurements, is a passive neutron measurement that determines the relative exposure of the set of fuel assemblies through the power functional relationship described in Sec. II. Using these two measurements, an inspector can obtain information rapidly about both the relative cooling time and the exposure of each fuel assembly, without interfering with the operator unnecessarily.

To determine the applicability of these two nondestructive techniques we used two experimental detector configurations. A square-ring detector capable

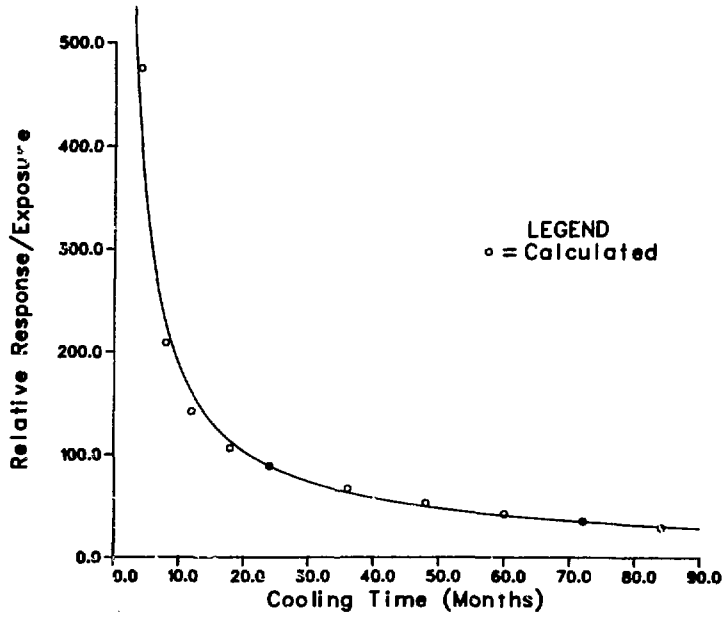

Fig. 3. Calculated response of dose divided by exposure as a function of cooling time for PWR fuel assemblies.

of measuring the gross gamma-ray and neutron signatures for each of the four sides of the irradiated fuel assemblies was fabricated. Figure 4 shows the components of the detector assembly. Four ^{235}U fission chambers (130 mg ^{235}U each) and four ionization chambers were mounted on the detector support ring

Fig. 4. Components of the square-ring detector.

and inserted into an aluminum watertight assembly. The inside dimension of the detector was 25.6 cm to allow easy insertion of PWR fuel assemblies with 20-cm widths (Fig. 5). The detector was attached to a fixture that was fitted to the fuel storage baskets used at the G. E. Morris Operation Spent-Fuel Storage Facility at Morris, Illinois. The detector could be placed on top of the storage racks at reactor storage basins.[14,16]

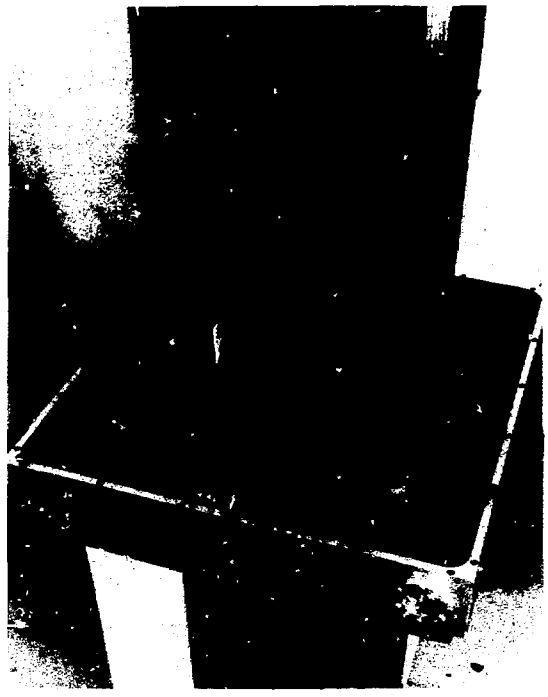

Fig. 5. Square-ring detector and an irradiated PWR fuel assembly.

The second measurement system consisted of a V-shaped positioning mechanism attached to a tube containing various gamma-ray and neutron detectors. The device was suspended from the wall in the receiving pool (Fig. 6). The fuel assembly was moved to the V-shaped positioning fixture, which automatically positioned the assembly correctly (Fig. 7) in less than a minute of the operator's time. The detector pipe was located at the corner of the fuel assembly to ensure a reproducible measurement geometry. The detector package consisted of

- an ion chamber to measure gross-gamma dose,
- a ^{235}U fission chamber ($\sim$130 mg ^{235}U) to measure the neutron emission rate, and
- a Be(γ,n) detector to record the high-energy (>1.66 MeV) gamma signature.[16]

Figure 8 shows a PWR fuel assembly in the measurement position.

The gamma-ray and neutron signals were recorded using two sets of electronics. The ion and neutron (ION-I) electronics unit records one gamma-ray and one neutron readout.[18] This battery-operated unit was developed for the IAEA inspectors. A microprocessor unit can read each of the four ion chambers and four fission chambers individually and simultaneously. The microprocessor system provides discrete information about the individual sides of the fuel

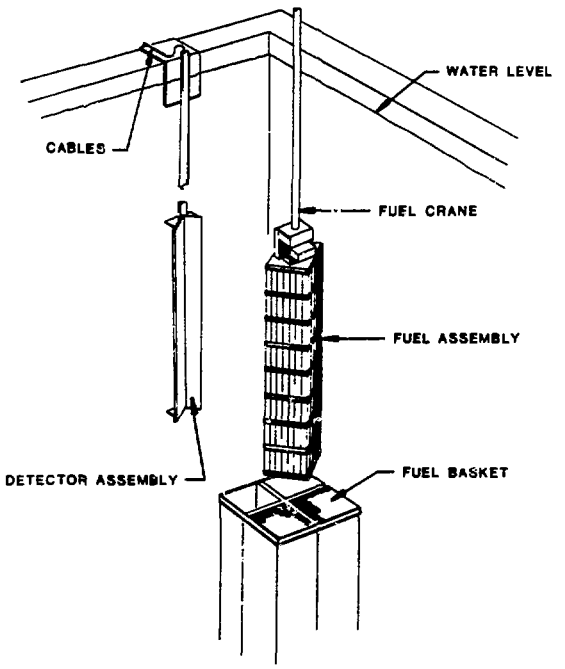

Fig. 6. Locating assembly with detector tube.

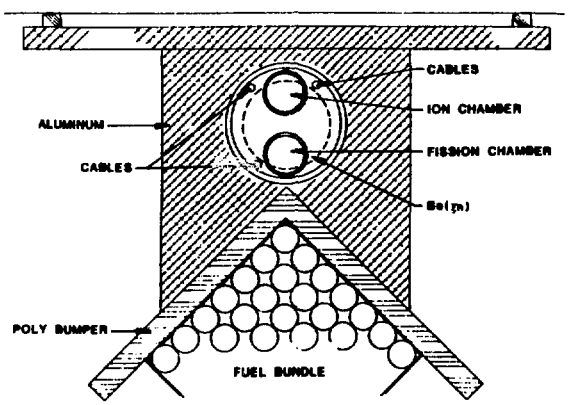

Fig. 7. Relative position of fuel assembly and detector tube and detector package used in V-detector.

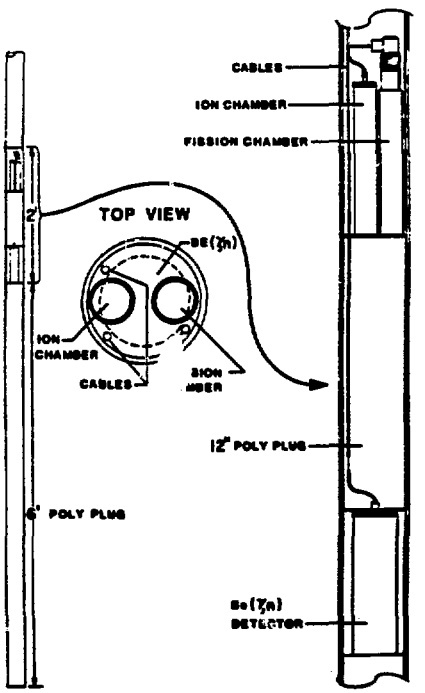

assembly, whereas the ION-I results are integral values for the side measurements.

IV. NEUTRON MEASUREMENTS

The square-ring detector described in Sec. III was evaluated at Los Alamos before being shipped to the G. E. Morris Operation Spent-Fuel Storage Facility for testing and evaluation with irradiated fuel assemblies. Measurements of the neutron detection sensitivity used a ^{252}Cf source underwater with and without the presence of an unirradiated fuel assembly. At the Morris Facility a variety of measurements demonstrated the applicability of this particular detector arrangement for the rapid and precise verification of irradiated fuel assemblies. These measurements included

Fig. 8. PWR fuel assembly located in positioning assembly for measurement.

- reproducibility measurements for estimation of precision,
- measurement of each side of an individual fuel assembly to determine the variability of source strengths,
- comparison with measurements using the two detector systems, and
- correlation between the measured neutron emission rates and the operator-declared values of exposure.

A. Evaluation of the Square-Ring Detector Using Calibrated Sources

For test purposes, the square-ring detector was placed in a cylinder (61.0-cm diam) filled with water. A minimum of 30 cm of water was above and below the detector. A polyethylene sheet was fabricated to hold a ^{252}Cf source at specified positions inside the detector. The positions were at 3.0-cm intervals, with nine positions available across the 26.04-cm inside distance. The ^{252}Cf-source strength was $3.75 \pm 0.01 \times 10^5$ n/s. Figure 9 shows

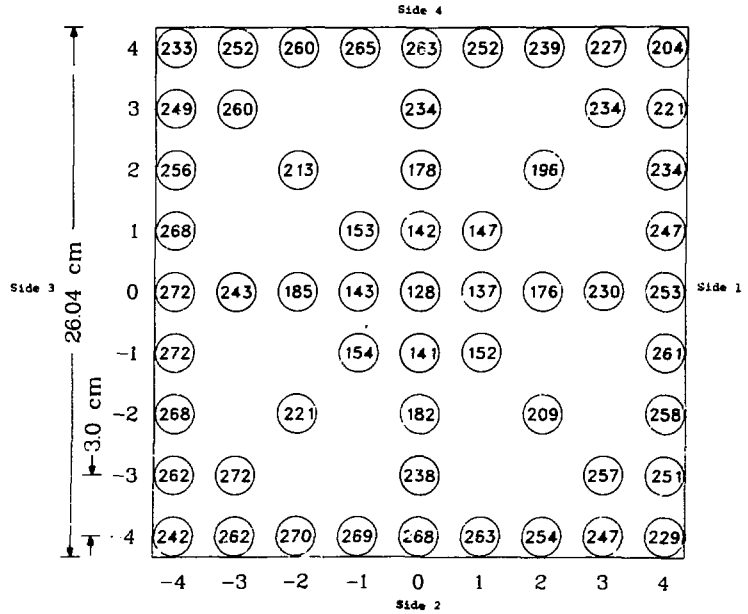

(a)

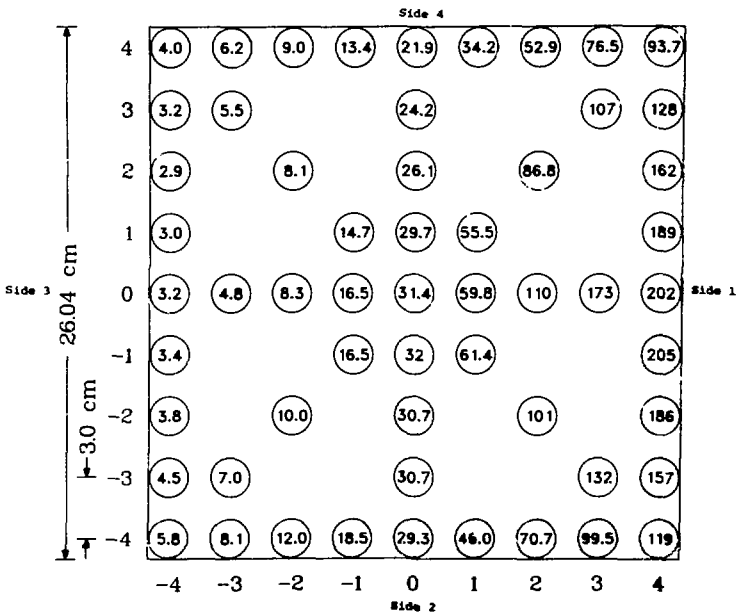

(b)

Fig. 9. Responses of a calibrated source at specified locations inside the square-ring detector for (a) all four detectors and (b) side 1 detector.

the measured results for one of the four detectors as well as the summation of the four detectors for the source in each of 57 positions. The threshold for each fission chamber was set at the minimum between the alpha pulse and the fission fragment signals. The numbers given at each location in Fig. 9 are the counts per second measured from the ^{252}Cf source. The counting precision for the data summing the four detectors was approximately 0.5%.

There appears to be a slight skew to the two-dimensional response, with the lower left-hand corner (between sides 2 and 3) being about 10% higher than the top right-hand corner (between sides 4 and 1). The fission chambers used in this detector had an active length of 12.5 cm and relative efficiencies within 0.6%. The effect of any detector skew is significantly reduced when the data for each detector are summed over all 57 source positions. When a fuel assembly is present, its effect upon source multiplication further reduces the effect of the skew.

Figure 10 shows the responses for each of the four detectors to the underwater movement of the source from the detector. The responses for each of the detectors were essentially identical. The source was moved from the detector along a line perpendicular to the axis of each detector.

These measurements showed the sensitivity of the square-ring detector to a calibrated ^{252}Cf source placed at specified x-y locations. The next step in the characterization of the detector was using a fuel assembly to introduce source multiplication and absorption.

B. Evaluation of the Square-Ring Detector Using a Simulated Fuel Assembly

An unirradiated 15 x 15 fuel assembly loaded with 3.2% ^{235}U-enriched fuel pins was placed in the water container. The square-ring detector was positioned to center the fuel assembly inside the detector. The fuel assembly contains 204 fuel pin positions and 21 guide-tube positions (Fig. 11). The ^{252}Cf source was placed into each of the 21 guide-tube positions at the

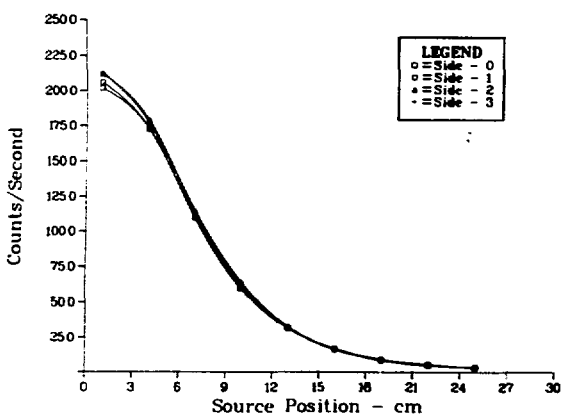

Fig. 10. Measured response of a source moved perpendicular to the axis of the detector.

vertical height corresponding to the midplane of the detector. Neutron emission rates were measured at each of the four fission chambers and were summed for the total response.

Figure 12 shows the results for the fuel assembly positioned at these different locations within the square-ring detector. The maximum detection efficiency was with the fuel assembly at the center of the square-ring detector; the minimum, with the fuel assembly in the corner. Maximum variability between the two sample locations was 27%.

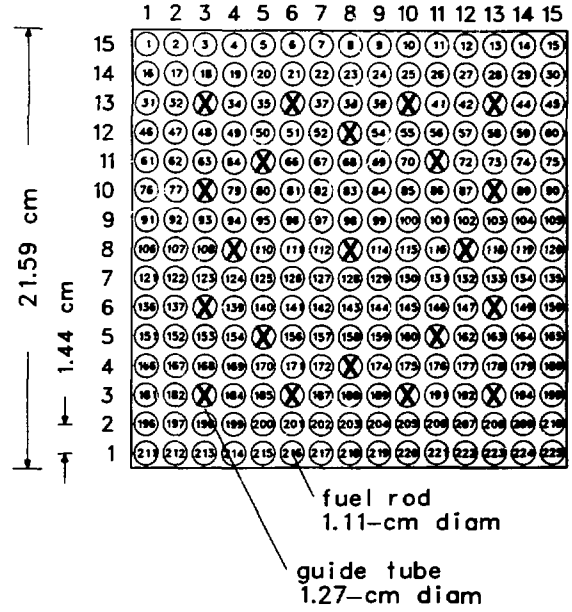

Fig. 11. Cross section of fuel assembly used in the simulated source measurements of a 15 x 15 PWR fuel assembly.

Three factors influence the measured variability in the detector-fuel assembly geometries described in Fig. 12:

(1) the distance between the detector and the fuel assembly (1/r effect),

(2) neutron absorption in the fuel assembly, and

(3) alteration of the thermalizing layer of water between the detector and fuel assembly.

As the fuel assembly is positioned against the side of the detector [(Fig. (12b)], the count rate should rise as a result of the 1/r effect; however, this effect is more than compensated for by factors (2) and (3). The fission chambers in the detector do not have any moderating material around them. A lower detection efficiency therefore results from the lack of any thermalizing moderator when the water is removed between the detector and the fuel assembly. The fuel assembly, which absorbs any neutron scattered back, reduces the counting efficiency by approximately 15% for the 12(b) case and 27% for the 12(c) case.

The axial sensitivity of the detector was measured by placing the fuel assembly at the center of the square ring and inserting the ^{252}Cf source into the center guide-tube position. The source was moved vertically, with the neutron emission rate being measured from 0 to 20 cm above the midplane of the detector. Figure 13 shows the measured results as a function of axial position.

the measured results for one of the four detectors as well as the summation of the four detectors for the source in each of 57 positions. The threshold for each fission chamber was set at the minimum between the alpha pulse and the fission fragment signals. The numbers given at each location in Fig. 9 are the counts per second measured from the ^{252}Cf source. The counting precision for the data summing the four detectors was approximately 0.5%.

There appears to be a slight skew to the two-dimensional response, with the lower left-hand corner (between sides 2 and 3) being about 10% higher than the top right-hand corner (between sides 4 and 1). The fission chambers used in this detector had an active length of 12.5 cm and relative efficiencies within 0.6%. The effect of any detector skew is significantly reduced when the data for each detector are summed over all 57 source positions. When a fuel assembly is present, its effect upon source multiplication further reduces the effect of the skew.

Figure 10 shows the responses for each of the four detectors to the underwater movement of the source from the detector. The responses for each of the detectors were essentially identical. The source was moved from the detector along a line perpendicular to the axis of each detector.

These measurements showed the sensitivity of the square-ring detector to a calibrated ^{252}Cf source placed at specified x-y locations. The next step in the characterization of the detector was using a fuel assembly to introduce source multiplication and absorption.

B. Evaluation of the Square-Ring Detector Using a Simulated Fuel Assembly

An unirradiated 15 x 15 fuel assembly loaded with 3.2% ^{235}U-enriched fuel pins was placed in the water container. The square-ring detector was positioned to center the fuel assembly inside the detector. The fuel assembly contains 204 fuel pin positions and 21 guide-tube positions (Fig. 11). The ^{252}Cf source was placed into each of the 21 guide-tube positions at the

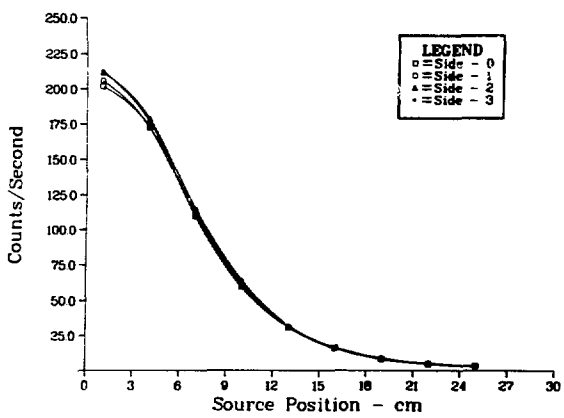

Fig. 10. Measured response of a source moved perpendicular to the axis of the detector.

vertical height corresponding to the midplane of the detector. Neutron emission rates were measured at each of the four fission chambers and were summed for the total response.

Figure 12 shows the results for the fuel assembly positioned at these different locations within the square-ring detector. The maximum detection efficiency was with the fuel assembly at the center of the square-ring detector; the minimum, with the fuel assembly in the corner. Maximum variability between the two sample locations was 27%.

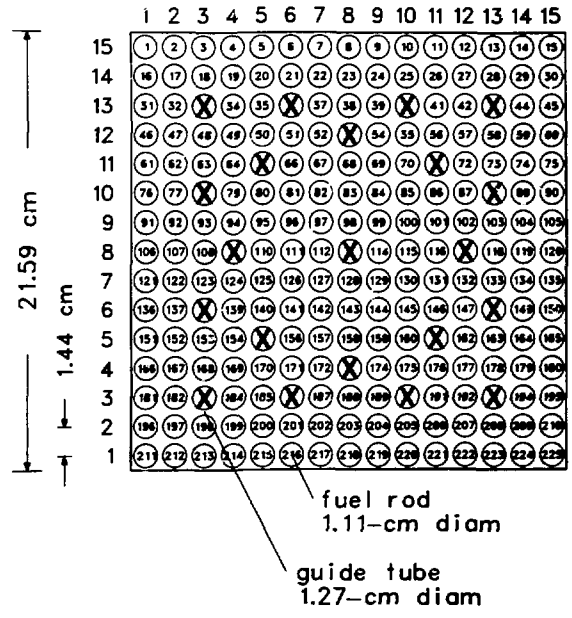

Fig. 11. Cross section of fuel assembly used in the simulated source measurements of a 15 x 15 PWR fuel assembly.

Three factors influence the measured variability in the detector-fuel assembly geometries described in Fig. 12:

(1) the distance between the detector and the fuel assembly (1/r effect),

(2) neutron absorption in the fuel assembly, and

(3) alteration of the thermalizing layer of water between the detector and fuel assembly.

As the fuel assembly is positioned against the side of the detector [(Fig. (12b)], the count rate should rise as a result of the 1/r effect; however, this effect is more than compensated for by factors (2) and (3). The fission chambers in the detector do not have any moderating material around them. A lower detection efficiency therefore results from the lack of any thermalizing moderator when the water is removed between the detector and the fuel assembly. The fuel assembly, which absorbs any neutron scattered back, reduces the counting efficiency by approximately 15% for the 12(b) case and 27% for the 12(c) case.

The axial sensitivity of the detector was measured by placing the fuel assembly at the center of the square ring and inserting the ^{252}Cf source into the center guide-tube position. The source was moved vertically, with the neutron emission rate being measured from 0 to 20 cm above the midplane of the detector. Figure 13 shows the measured results as a function of axial position.

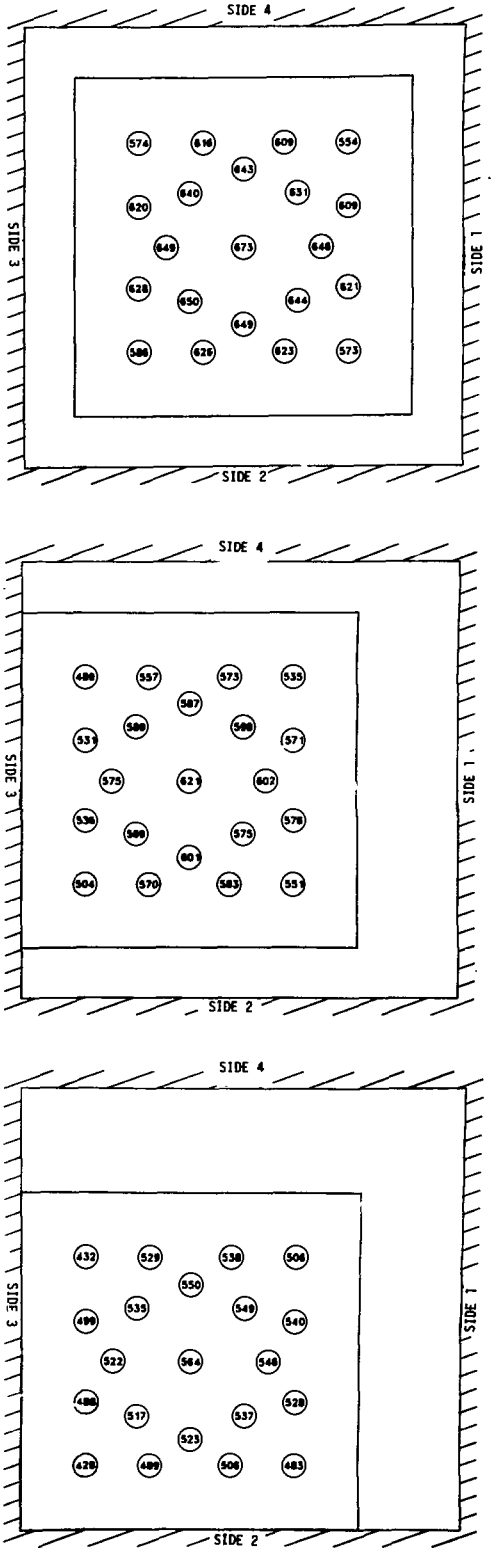

Fig. 12. Measured neutron rates (count/s) for the ^{252}Cf in the 21 guide-tube positions for three different measurement geometries.

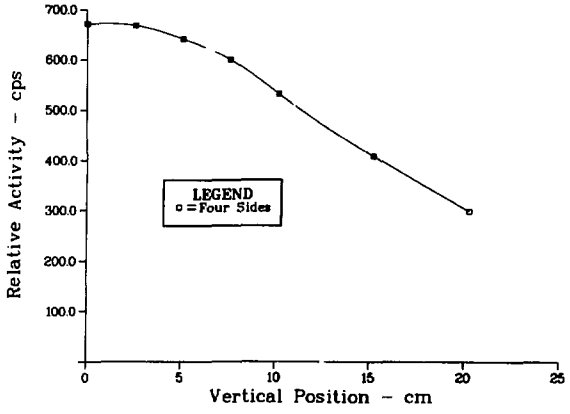

Fig. 13. Measured neutron rates for a ^{252}Cf source in the center guide-tube position at specified vertical position.

At 5.0 cm above the detector's midplane the detector's response is 95.5% of the source at the midplane. A 74% contribution still exists at the 20-cm vertical position.

These measurements show that the position sensitivity of the detector is reduced by the effects of neutron multiplication and absorption upon neutron sources. The square ring measured an extended region of the fuel assembly, about 40 cm long.

C. Measurement of Irradiated PWR Fuel Assemblies

A series of nondestructive neutron and gamma-ray measurements was performed on a set of 14 PWR fuel assemblies with exposures ranging from 18.4 to 40.6 GWd/tU. These fuel assemblies were irradiated in a 450-MWe Westinghouse-type PWR. Table IV lists the fuel parameters of each assembly.

Each of the 14 fuel assemblies listed in Table V was placed in the square-ring detector that measured each side simultaneously. Both the neutron emission rate and gross gamma-ray dose were recorded using two data acquisition systems, the ION-1 electronics unit and the microprocessor unit.

A second measurement was also performed on each fuel assembly using the V-shaped positioning device[14] with a fission and ion chamber that measured the neutron emission rates and gross gamma-ray doses at the corner of the fuel assembly. Both of these detectors were placed in a vertical direction as opposed to the horizontal orientation of the fission and ion chambers in the square-ring detector.

TABLE IV

FUEL ASSEMBLY PARAMETERS FOR 14 x 14 ARRAY

Fuel Assembly	
Width (cm)	19.7
Length (cm)	366.0
Upper fuel assembly (kg)	443.7

Fuel Rod	
Diameter (cm)	0.93
^{235}U enrichment (%)	3.04-3.40
Cladding	Zircaloy

TABLE V

FUEL ASSEMBLIES MEASURED AT THE MORRIS SPENT-FUEL STORAGE FACILITY

Fuel Assembly	Discharge Date	Time Since Discharge (Days)	Initial ^{235}U Enrichment (%)	Declared Exposure (GWd/tU)
A-72	10/16/74	2445	3.40	18.47
A-54	10/16/74	2445	3.40	20.81
A-74	10/16/74	2445	3.40	20.84
A-73	10/16/74	2445	3.40	20.91
D-31	11/16/75	2049	3.04	23.43
C-32	4/6/74	2638	3.40	23.57
D-26	11/16/75	2049	3.04	26.91
C-51	2/26/76	1947	3.40	28.90
B-52	2/26/76	1947	3.02	31.71
C-52	3/4/77	1575	3.40	32.82
C-70	3/4/77	1575	3.04	33.08
C-72	3/4/77	1575	3.04	37.85
C-56	3/4/77	1575	3.40	40.07
C-64	3/4/77	1575	3.40	40.55

The square-ring detector was mounted onto a support bracket (Fig. 14) atop the fuel assembly storage basket used at the facility. Each fuel assembly was first lowered into the square-ring detector with each of the four sides being measured at designated axial positions; then the fuel assembly was moved to the V-detector with each corner being measured separately. This process was repeated for each of the 14 irradiated fuel assemblies.

1. Relationship Between Neutron Emission Rate and Exposure. As was discussed earlier in Sec. II, the neutron source strength varies as a function of exposure by the following equation:

$$\text{Count Rate} = \alpha * \text{Exposure}^{\beta} \quad , \tag{2}$$

where α is a scaling parameter and β ranges in value between 2.8 and 4.0 depending upon the fuel being measured. This power function relationship has been verified experimentally for a variety of fuel assemblies.[7,14,16,19]

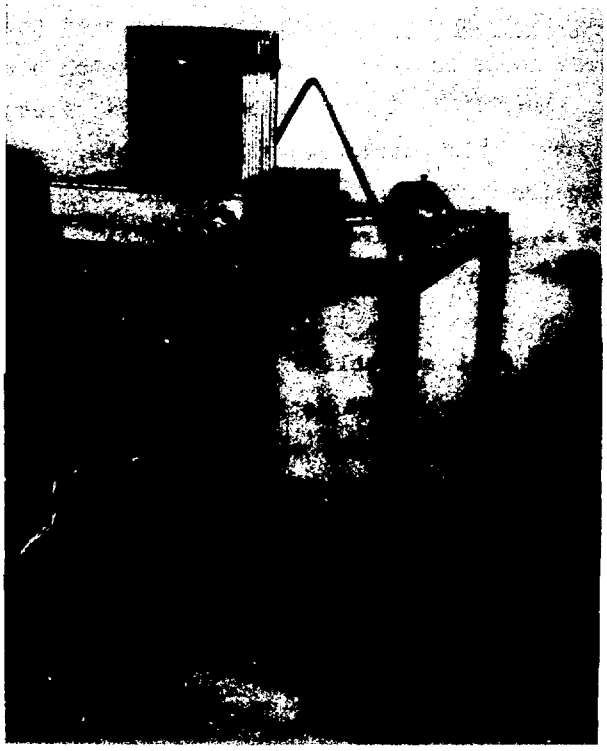

Fig. 14. Square-ring detector, mounted on support bracket, on top of the PWR storage baskets.

2. Reproducibility Measurements. To demonstrate electronic stability and freedom from positioning problems, a series of repeated measurements was performed. The fuel assembly C-32 (23.57 GWd/tU) was our standard. It was lowered into the square-ring detector until the midplane of the assembly was positioned at the detector. Measurements of the neutron emission rate and gross gamma-ray dose for each side were recorded. After the fuel assembly was removed from the square ring and moved away from the storage basket, it was returned and repositioned in the detectors to check reproducibility. This process simulated independent measurements and measured the precision of the entire process (Table VI). For a set of seven measurements, the average deviation was 0.6% for the neutron measurements. The gamma-ray dose measurements agreed even better, with a 0.2% precision. At the beginning of each day's measurements, we remeasured the C-32 fuel assembly. Over a 6-day period the neutron measurements varied an average of 1.5% (Table VII); gamma-ray dose measurements varied by 1.3%. Variation in the reproducibility can be divided into two components, uncertainty in the repositioning of the fuel assembly and changes in the counting electronics. (This is discussed in Sec. IV.C.6.) Measurement variation can be related about equally to accurate repositioning of the fuel assembly and the counting statistics.[20]

3. Variability in Source Strength at One Axial Location. Measured neutron emission rates can vary by as much as 30 to 40%, depending upon which side or corner of a fuel assembly is measured.[14,20] These asymmetries in source strength can be related to specific irradiation histories. For example, positioning near the core periphery during the first cycle of an assembly can create a gradient that persists throughout the lifetime of the assembly.[20] This asymmetry in neutron emission rates can complicate data interpretation by introducing another geometric variable.

Each of the four sides of the 14 fuel assemblies was measured (Table VIII). The measured neutron activities were corrected back to the time of discharge from the reactor using the 18.1-yr half-life of ^{244}Cm as the time factor. As discussed in Sec. II.C, ^{244}Cm is the principal source of neutrons in fuel assemblies with exposures above 10 GWd/tU (Fig. 1). The second most important source of neutrons is ^{242}Cm, which has a relatively short half-life ($t_{1/2}$ = 0.446 yr). In this particular set of fuel assemblies, the shortest cooling time since discharge from the reactor was 1575 days; therefore, only

TABLE VI

SQUARE-RING REPRODUCIBILITY MEASUREMENTS

Measurement	Fission Chamber[a]					Ion Chamber				
	Side 1	Side 2	Side 3	Side 4	Total	Side 1	Side 2	Side 3	Side 4	Total
	5133	3690	4341	6590	19 754	562	395	412	543	1912
1	5276	3701	4442	6831	20 250	561	394	412	544	1911
	5004	3774	4302	6878	18 958	555	368	417	559	1917
2	5018	3635	4356	6754	19 763	555	386	417	559	1917
	5093	3597	4375	7088	20 153	561	378	411	570	1920
3	5080	3535	4293	6885	19 793	562	378	411	571	1922
	5136	3784	4338	6939	20 197	571	398	407	541	1917
4	5180	3694	4387	6901	20 162	571	399	407	541	1918
	5087	3680	4193	7036	19 996	571	382	405	564	1922
5	5153	3607	4289	7007	20 056	572	382	404	565	1923
	5075	3456	4222	7043	19 796	580	382	399	565	1926
6	5179	3693	4198	6844	19 914	580	382	399	564	1925
	5143	3651	4307	6987	20 088	568	380	408	567	1923
7	5021	3616	4289	6830	19 756	571	379	405	567	1922
Average			19 974 ± 112 (0.6%)					1919 ± 4.7 (0.2%)		

[a] We used 60-s counts on fuel assembly C-32 (23.57 GWd/tU).

TABLE VII

LONG-TERM REPRODUCIBILITY MEASUREMENTS

	Fission Chamber[a]					Ion Chamber				
Date	Side 1	Side 2	Side 3	Side 4	Total	Side 1	Side 2	Side 3	Side 4	Total
6/25/81	5113	3651	4309	6901	19 974	567	386	408	558	1919
6/26/81	5146	3697	4482	6950	20 275	574	400	431	579	1984
6/27/81	5211	3849	4332	6860	20 252	578	415	428	556	1977
6/28/81	5308	3896	4413	6404	20 021	597	444	416	520	1977
6/29/81	5152	3748	4252	6913	20 065	610	410	408	563	1991
6/30/81	5453	3964	4432	6942	20 773	596	420	412	548	1976
Average					20 227 ± 295 (1.5%)					1971 ± 26 (1.3%)

[a] We used 60-s counts on fuel assembly C-32 (23.57 GWd/tU).

TABLE VIII

MEASURED NEUTRON RESULTS FOR THE SQUARE-RING DETECTOR

Fuel Assembly	Declared Exposure (GWd/tU)	Measured Activity[a] (Counts/s)				
		Side 1	Side 2	Side 3	Side 4	Total[b]
A-72	18.47	101	72	80	109	362
A-54	20.81	137	132	161	176	606
A-74	20.84	135	141	152	166	594
A-73	20.91	140	133	154	171	598
D-31	23.43	134	152	187	161	634
C-32	23.57	115	86	100	159	460
D-26	26.91	209	195	262	308	974
C-51	28.90	209	216	293	323	1045
B-52	31.71	456	436	491	569	1952
C-52	32.82	524	397	374	541	1836
C-70	33.08	365	432	573	563	1933
C-72	37.85	700	605	711	910	2926
C-56	40.07	790	780	939	1056	3565
C-64	40.55	868	855	917	1016	3656

[a]All the measured rates were corrected to time of discharge from the reactor using the 18.1-yr half-life of ^{244}Cm.

[b]Measurement precisions were better than 1% for all fuel assemblies.

0.12% of the ^{242}Cm present at time of discharge would still be present at the time of measurement.

Figure 15 shows a plot of the individual measurements for each side of the fuel assemblies. Maximum variability occurs for fuel assembly C-32, which varies from -25 to +24% of its average value. The measurements of the fuel assemblies varied significantly from their average values.

Table IX gives similar measured neutron results for the corner V-detector. Figure 16 shows that the C-32 and C-72 fuel assemblies again have the maximum variability with C-32 varying from -22 to +28% and C-72 varying from -12 to +13%. In Sec. IV.C.5, we quantify the effect of this angular variability upon the verification of exposure of the individual fuel assemblies.

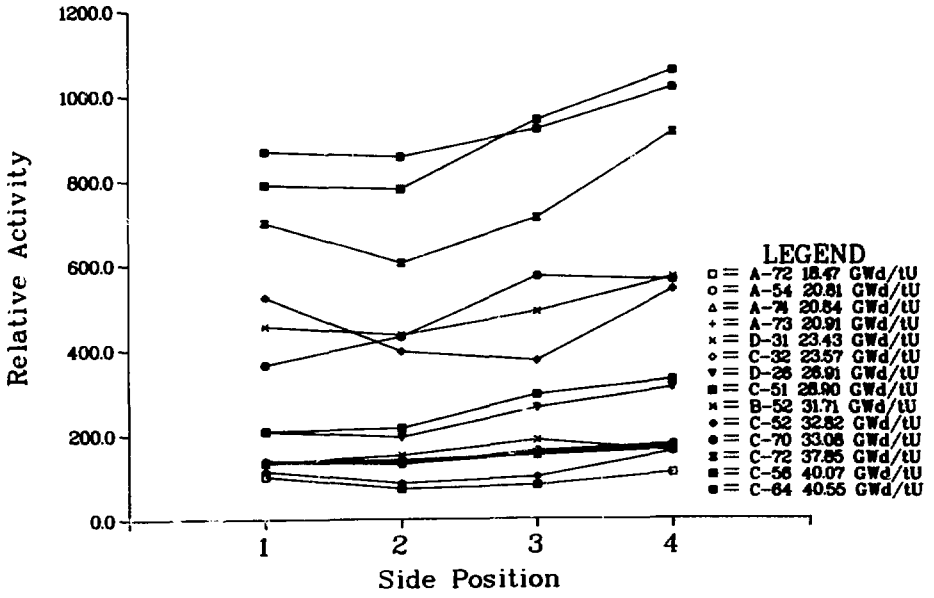

Fig. 15. Measured neutron activities for each side of the 14 irradiated fuel assemblies. The count rates were corrected to time of discharge using the 18.1-yr half-life of ^{244}Cm.

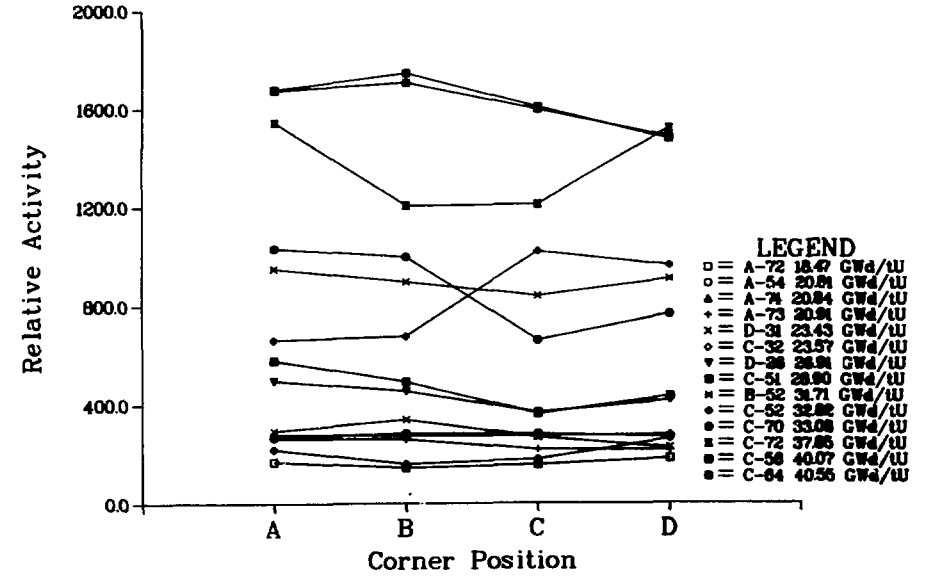

Fig. 16. Measured neutron activities for each corner of the 14 irradiated fuel assemblies. The count rates were corrected to time of discharge using the 18.1-yr half-life of ^{244}Cm.

TABLE IX

MEASURED NEUTRON RESULTS FOR THE CORNER V-DETECTOR

Fuel Assembly	Declared Exposure (GWd/tU)	Measured Activity[a] (Counts/s)				
		Corner A	Corner B	Corner C	Corner D	Total[b]
A-72	18.47	167	143	155	180	645
A-54	20.81	267	281	278	268	1094
A-74	20.84	277	273	272	276	1094
A-73	20.91	263	258	216	215	952
D-31	23.43	292	338	266	224	1120
C-32	23.57	218	159	177	260	814
D-26	26.91	498	455	367	416	1736
C-51	28.90	580	493	361	433	1867
B-52	31.71	949	896	839	908	3592
C-52	32.82	662	676	1021	963	3322
C-70	33.08	1032	998	660	765	3455
C-72	37.85	1543	1204	1210	1520	5477
C-56	40.07	1677	1743	1606	1476	6502
C-64	40.55	1674	1705	1596	1485	6460

[a]All the measured rates were corrected to time of discharge from the reactor using the 18.1-yr half-life of ^{244}Cm.

[b]Measurement precisions were better than 1% for all fuel assemblies.

4. Axial Neutron Profiles. The axial neutron profiles were measured for four fuel assemblies with declared exposures ranging from 18.47 to 31.71 GWd/tU. The neutron emission rates were measured at 30-cm intervals over the active fuel region. Figure 17 shows the axial profiles for each of the four sides of the fuel assemblies. As noted in Table VIII and Fig. 15, the neutron signal varies considerably from one side to another. The effect of the differences in the neutron emission rates is discussed in Sec. II.C.5.

These measurements demonstrate the relatively flat profile through the central regions of each fuel assembly. All of our subsequent measurements were performed in the -60- to +60-cm region.

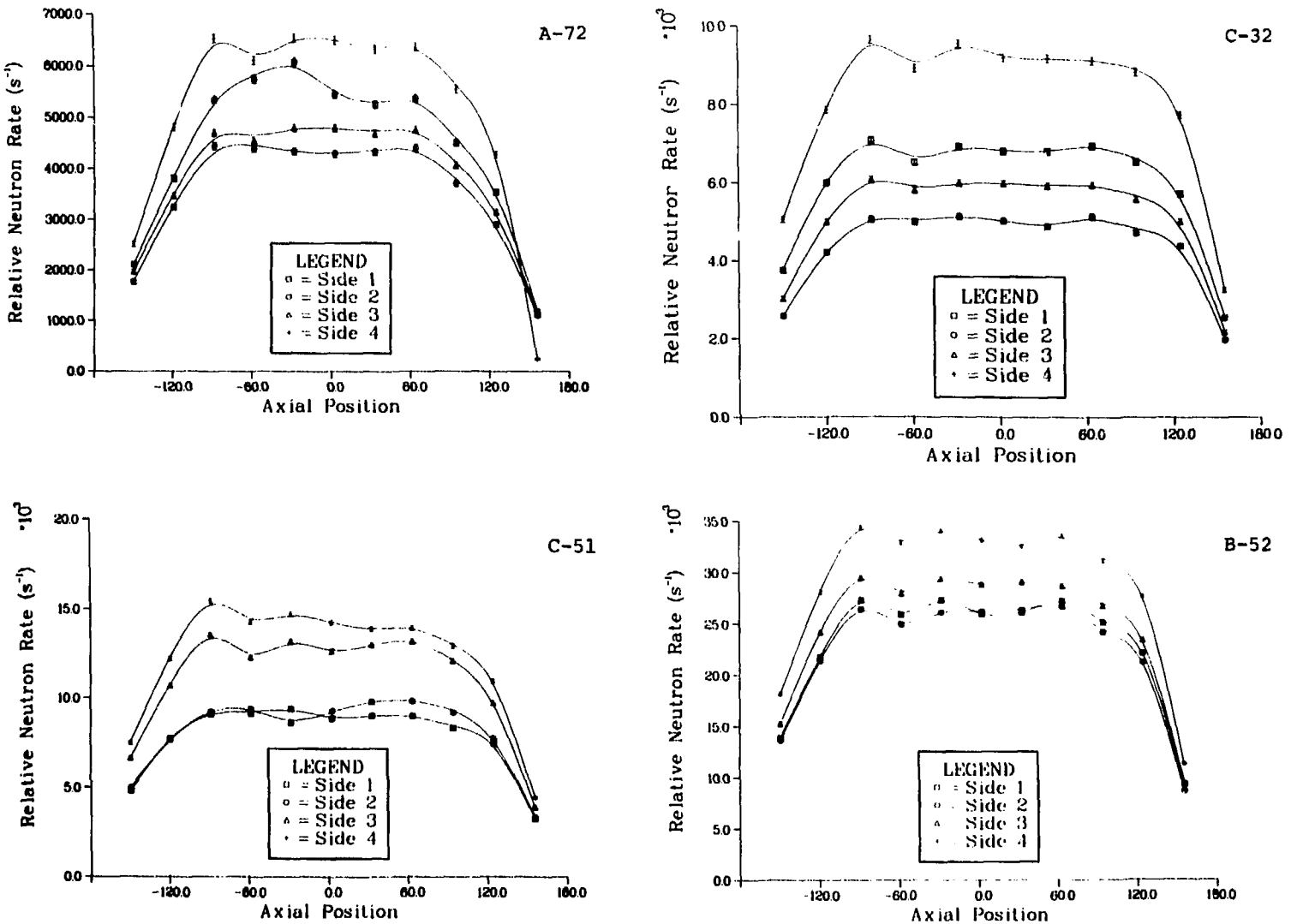

Fig. 17. Axial neutron profiles for each side of the four fuel assemblies: A-72 (18.47 GWd/tU), C-32 (23.57 GWd/tU), C-51 (28.90 GWd/tU), and B-52 (31.71 GWd/tU).

5. Correlation Between Measured Neutron Rates and Declared Exposures. We evaluated the use of a power functional relationship for correlating the measured neutron emission rates of irradiated fuel assemblies with operator-declared values of exposure. The total neutron rates vs operator-declared values of exposure are plotted in Fig. 18. The average difference between the least squares fitted line and the declared values was 4.2%. Similar results were obtained when data from only one side at a time were used in the analysis (Table X). Average absolute differences ranged between 3.6 and 6.3% for the individual side measurements.

Similar results were obtained using the corner V-detector (Fig. 19 and Table XI) with the average absolute differences ranging from 4.3 to 6.6% for the individual corner measurements and being 4.1% for the summed data.

Table XII presents comparisons of the two detector systems and evaluates various combinations of detector arrangements. The first set for the side measurements includes the data from Table X, in which only one side detector was analyzed. The second set gives the results for fission chambers placed on opposite sides of the fuel assembly to simulate a "fork" detector. The third set simulates a V-shaped detector with horizontal fission chambers. A three-sided detector arrangement corresponds to the fourth set, and a square ring-detector corresponds to the fifth set. The average differences range from 3.6 to 6.3% without regard to the detector measurement geometry. Results for the corner measurements were very similar with the differences ranging from 4.3 to 6.6%. For each type of detector, the average percentage difference appears to improve as we move from one detector to two detectors on adjacent sides or corners, to three detectors, to two detectors on opposite sides or corners, and to four detectors.

We have already discussed the variability of measurements at one axial position for the same fuel assembly. If we use the power functional relationship obtained from the four sides or four corners, we then can use the maximum variability in the count rates to determine the maximum difference in the calculated exposures. In Table XIII the four assemblies with the maximum variability in count rates demonstrate the magnitude of their effect. Table XIII shows that the average error introduced would be in the range of 7 to 8%. Because the operator-declared values are only accurate within 4 to 6%,[16] single measurements on one side or one corner would be nearly as accurate. However, measuring all four sides (or corners) or opposite sides cancels some of the

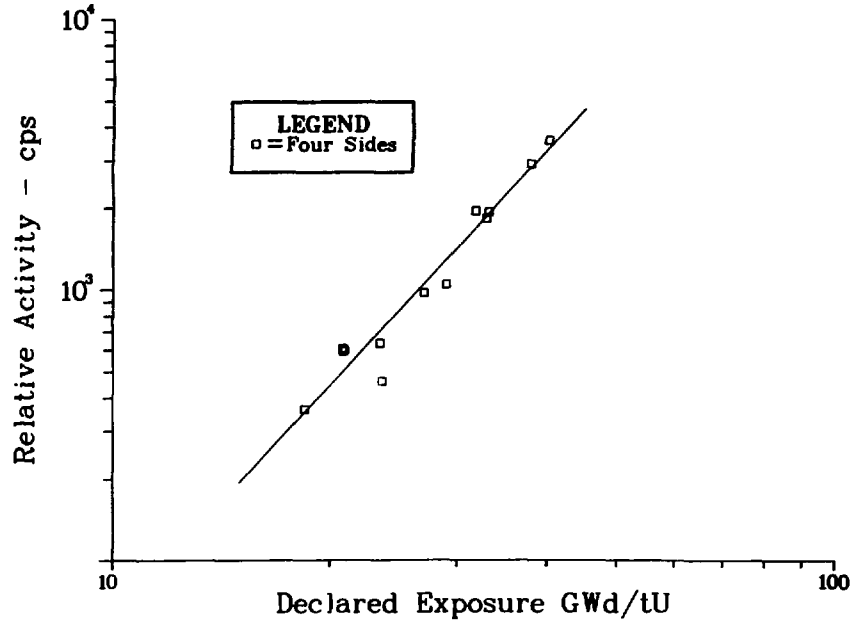

Fig. 18. Measured neutron emission rates using the square-ring detector values vs the operator-declared exposure values for 14 PWR fuel assemblies.

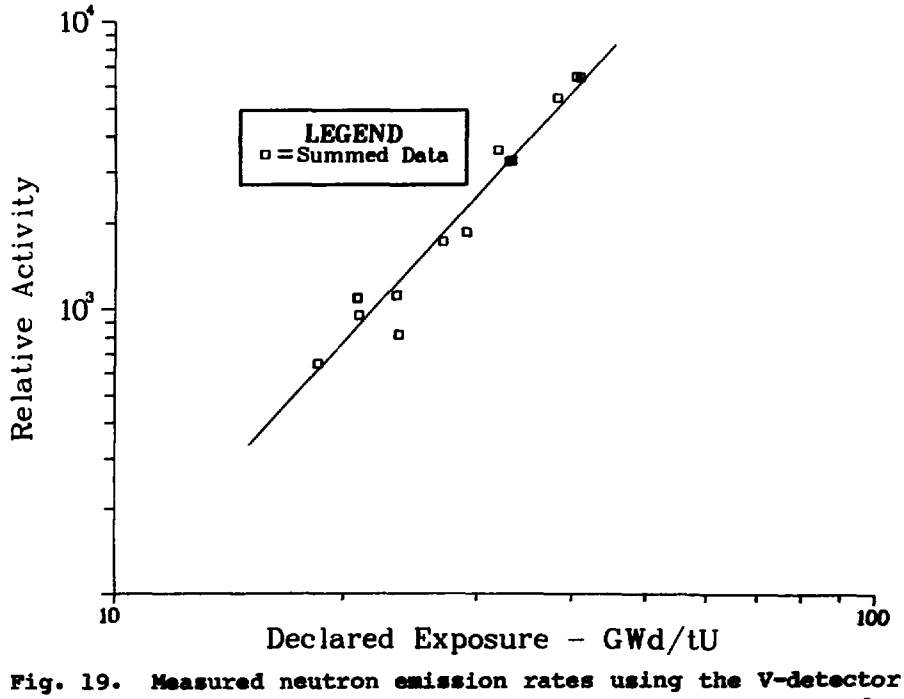

Fig. 19. Measured neutron emission rates using the V-detector values vs the operator-declared exposure values for 14 PWR fuel assemblies.

TABLE X

RELATIVE RESULTS BASED ON THE SQUARE-RING MEASUREMENTS

Fuel Assembly	Declared Exposure (GWd/tU)	Calculated Values				
		Side 1	Side 2	Side 3	Side 4	Average
A-72	18.47	19.72	18.19	17.82	18.76	18.61
A-54	20.81	21.96	22.36	22.64	22.13	22.24
A-74	20.84	21.85	22.87	22.20	21.68	22.09
A-73	20.91	22.13	22.42	22.30	21.91	22.14
D-31	23.43	21.79	23.46	23.83	21.46	22.59
C-32	23.57	20.64	19.32	19.23	21.37	20.22
D-26	26.91	25.50	25.54	26.74	26.82	26.20
C-51	28.90	25.50	26.45	27.88	27.38	26.84
B-52	31.71	33.61	33.61	33.16	33.12	33.31
C-52	32.82	35.31	32.55	30.21	32.55	32.61
C-70	33.08	31.07	33.50	34.96	33.00	33.20
C-72	37.85	39.12	37.58	37.64	38.93	38.31
C-56	40.07	40.83	40.98	41.40	40.97	41.01
C-64	40.55	42.21	42.28	41.07	40.43	41.37
Average absolute difference (%)		6.3	5.2	5.2	3.6	4.2
Power function parameter[a]						
	R^2	0.9296	0.9248	0.9266	0.9671	0.9527
	α	0.02213	0.01456	0.01776	0.02161	0.07622
	β	2.826	2.933	2.921	2.908	2.985

[a] R^2 is the correlation coefficient. When multiplied by 100, it represents the percentage of the total mean variation explained by the regression.

TABLE XI

RELATIVE RESULTS BASED ON THE CORNER V-DETECTOR MEASUREMENTS

Fuel Assembly	Declared Exposure (GWd/tU)	Calculated Values				
		Corner A	Corner B	Corner C	Corner D	Average
A-72	18.47	18.63	18.07	18.93	19.39	18.73
A-54	20.81	21.83	22.68	23.08	22.24	22.40
A-74	20.84	22.10	22.46	22.91	22.47	22.43
A-73	20.91	21.72	22.03	21.19	20.61	21.37
D-31	23.43	22.50	24.13	22.74	20.91	22.59
C-32	23.57	20.39	18.73	19.80	22.01	20.27
D-26	26.91	26.94	26.66	25.37	25.89	26.20
C-51	28.90	28.37	27.39	25.23	26.25	26.86
B-52	31.71	33.49	33.48	33.60	33.89	33.53
C-52	32.82	29.66	30.45	30.92	34.58	32.65
C-70	33.08	34.45	34.71	30.97	31.94	33.09
C-72	37.85	39.46	36.97	38.05	40.48	38.69
C-56	40.07	40.59	41.87	41.90	40.07	41.00
C-64	40.55	40.56	41.56	41.81	40.16	40.91
Average absolute difference (%)		4.3	5.8	6.6	5.4	4.1
Power function parameters[a]						
R^2		0.9531	0.9138	0.9087	0.9445	0.9524
α		0.02875	0.02597	0.02707	0.03342	0.11432
β		2.963	2.976	2.942	2.898	2.948

[a] R^2 is the correlation coefficient. When multiplied by 100, it represents the percentage of the total mean variation explained by the regression.

TABLE XII

COMPARISON OF THE TWO MEASUREMENT GEOMETRIES

Data Set	Measurement	R^2	Parameter Value α	β	Average Difference (%)
1	Side 1	0.9296[a]	0.02213	2.826	6.3
	Side 2	0.9248	0.01456	2.933	5.2
	Side 3	0.9266	0.01776	2.921	5.2
	Side 4	0.9671	0.02161	2.908	3.6
2	Sides 1 and 3	0.9471	0.03964	2.876	4.3
	Sides 2 and 4	0.9569	0.03663	2.915	4.1
3	Sides 1 and 2	0.9357	0.03663	2.874	5.4
	Sides 2 and 3	0.9295	0.03218	2.928	5.2
	Sides 3 and 4	0.9584	0.03993	2.911	4.0
	Sides 4 and 1	0.9566	0.04332	2.873	4.7
4	Sides 1, 2, and 3	0.9412	0.05416	2.892	4.5
	Sides 2, 3, and 4	0.9516	0.05455	2.916	4.3
	Sides 3, 4, and 1	0.9579	0.06150	2.886	4.0
	Sides 4, 1, and 2	0.9530	0.05833	2.887	4.6
5	All four sides	0.9527	0.07622	2.895	4.2
	Corner Measurement				
1	Corner A	0.9513	0.02876	2.963	4.3
	Corner B	0.9138	0.02597	2.976	5.8
	Corner C	0.9087	0.02707	2.942	6.6
	Corner D	0.9445	0.03342	2.898	5.4
2	Corners A and C	0.9499	0.05436	2.963	4.3
	Corners B and D	0.9544	0.06011	2.933	4.1
3	Corners A and B	0.9390	0.05498	2.968	4.6
	Corners B and C	0.9264	0.05226	2.965	4.8
	Corners C and D	0.9356	0.06062	2.919	5.8
	Corners D and A	0.9628	0.06160	2.933	4.0
4	Corners A, B, and C	0.9432	0.08046	2.967	4.3
	Corners B, C, and D	0.9446	0.08650	2.939	4.7
	Corners C, D, and A	0.9543	0.08795	2.940	4.5
	Corners D, A, and B	0.9571	0.08838	2.945	4.2
5	All four corners	0.9524	0.11432	2.948	4.1

[a] R^2 is the correlation coefficient. When multiplied by 100, it represents the percentage of the total mean variation explained by the regression.

TABLE XIII

EFFECT OF VARIABILITY IN COUNTING RATES ON CALCULATED EXPOSURES USING THE POWER FUNCTIONAL RELATIONSHIP

Fuel Assembly Measurements	GWd/tU	Range in Measured Activities (Counts/s)	Range in Calculated Exposures (GWd/tU)	Difference (%)
Side				
C-32	18.47	86 - 159	18.30 - 22.63	-1.0 to 22.5
C-70	33.08	365 - 573	30.14 - 35.23	-8.9 to 6.5
C-72	37.85	605 - 910	35.89 - 41.33	-5.2 to 9.2
C-56	40.07	780 - 1056	39.19 - 43.51	-2.2 to 8.6
			Average	8.0
Corner				
C-32	18.47	159 - 260	18.64 - 22.02	5.5 to 19.2
C-70	33.08	660 - 1032	30.21 - 35.16	-8.7 to 6.3
C-72	37.85	1210 - 1543	37.11 - 40.30	-2.0 to 6.5
C-56	40.07	1476 - 1677	39.69 - 41.45	-10 to 3.4
			Average	6.6

assembly-positioning uncertainties. Positioning was controlled better in the present work than we could expect under normal inspection conditions. Thus, the single side (or corner) results look better than might be the normal case.

6. Position Sensitivity for the Square-Ring Detector. To determine the position sensitivity of the fuel assembly within the square-ring detector, fuel assembly B-52 (31.71 GWd/tU) was positioned at 11 different locations, and the neutron rates were measured for each of the four fission chambers. These positions varied from the center, to the side, to the corners to obtain the maximum count rate changes (Table XIV).

The count rates for a specific fission chamber could vary significantly (698.8 to 989.3 counts/s for side 1); however, the total counts for all four sides varied only an average of 3.7%. Part of this variation is due to a decrease in the fission counter efficiency from water displacement as the

TABLE XIV

POSITION SENSITIVITY FOR NEUTRON MEASUREMENTS USING THE SQUARE-RING DETECTOR[a]

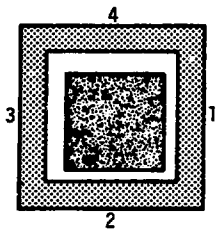

Side 1 925.7
Side 2 942.9
Side 3 899.0
Side 4 894.3

Total 3661.9

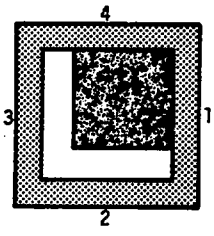

Side 1 950.3
Side 2 758.8
Side 3 739.3
Side 4 919.3

Total 3367.7

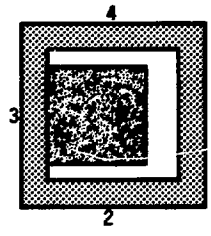

Side 1 723.4
Side 2 882.9
Side 3 915.1
Side 4 885.8

Total 3407.2

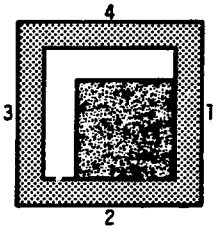

Side 1 977.0
Side 2 959.9
Side 3 789.6
Side 4 768.1

Total 3494.6

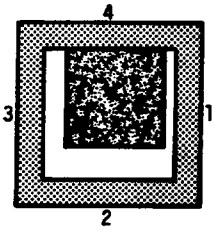

Side 1 912.0
Side 2 770.7
Side 3 855.3
Side 4 930.9

Total 3469.9

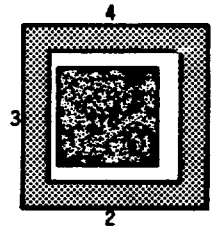

Side 1 857.7
Side 2 931.4
Side 3 923.2
Side 4 882.6

Total 3594.8

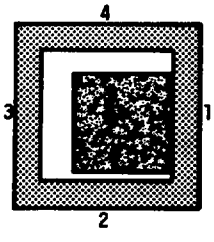

Side 1 984.5
Side 2 930.0
Side 3 782.8
Side 4 883.4

Total 3580.7

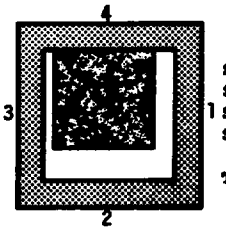

Side 1 719.4
Side 2 760.2
Side 3 895.6
Side 4 916.2

Total 3291.4

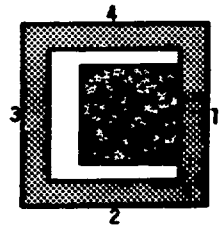

Side 1 989.3
Side 2 923.3
Side 3 810.5
Side 4 852.2

Total 3575.3

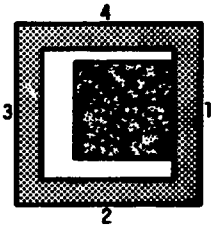

Side 1 964.1
Side 2 781.6
Side 3 747.0
Side 4 916.3

Total 3409.0

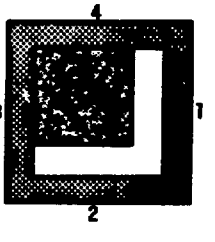

Side 1 698.8
Side 2 766.6
Side 3 897.9
Side 4 921.1

Total 3284.4

Average total 3467.8 ± 126.8
(3.7%)

[a]Results are given in counts per second. These results were taken using the ICM-1 electronics package with a threshold setting of 24.

assembly is moved next to the side wall of the square ring. Polyethylene and cadmium will be placed around each detector in future models to eliminate this effect.

V. GROSS GAMMA MEASUREMENTS

The capacity of the square-ring detector to measure simultaneously the gross gamma-ray doses from the four sides of an irradiated fuel assembly was evaluated at the Morris Facility. Measurements similar to those described in Sec. IV included the following.

- Reproducibility measurements for estimation of precision.
- Measurement of each side of an individual fuel assembly to determine the variability of source strengths.
- Comparison with measurements using the two detector system.
- Correlation between the declared cooling time and the measured dose.

Both the ION-1 electronics unit and the microprocessor unit recorded the data. The responses of the ion chambers were not calibrated and therefore are only relative numbers. From prior work we have established that the ion chambers do operate linearly, that is, a twofold increase in gross gamma-ray activity results in a twofold increase in the measured signal.

A. Origins of Gross Gamma-Ray Sources

Table XV lists the fission product and activation product isotopes that are the principal sources of the gross gamma-ray signal in irradiated fuel assemblies. Two of the shielded isotopes, ^{134}Cs and ^{154}Eu, are produced primarily through a secondary reaction. They are not produced primarily by fission but rather by fission followed by one or more neutron captures. Because of complicated production chains, different half-lives, and different fission yields, it is extremely difficult to relate the gross gamma-ray doses to operator-declared exposures.

B. Reproducibility Measurements

Repeated measurements of the C-32 irradiated fuel assembly gave a precision of 1.3%, which is slightly better than the comparable precision of the neutron measurements (Tables VI and VII).

TABLE XV

MEASURABLE ISOTOPES IN TYPICAL LWR FUEL ASSEMBLIES

Fission Product		Fission Yield (%)		Gamma-Ray Energy (keV) [Branching Ratio]
Isotope	Half-Life	^{235}U	^{239}Pu	
^{137}Cs	30.17 yr	6.222	6.689	661.6 [0.851]
^{154}Eu[a]	8.5 yr	2.69-6[b]	9.22-5	1274.4 [0.355], 1004.8 [0.174], 996.3 [0.103]
^{125}Sb	2.71 yr	0.0294	0.1110	427.9 [0.30], 600.8 [0.18], 686.2 [0.12], 463.5 [0.11]
^{134}Cs[a]	2.062 yr	1.27-5	9.89-4	604.7 [0.976], 795.8 [0.854], 801.8 [0.087], 1365.1 [0.0304], 1167.9 [0.018]
^{106}Ru-Rh	366.4 days	0.4018	4.280	622.2 [0.098], 1050.5 [0.016]
^{144}Ce-Pr	284.5 days	5.475	3.736	696.5 [0.0134], 2185.6 [0.0066], 1489.2 [0.0026]
^{95}Zr	63.98 days	6.496	4.892	756.7 [0.546], 724.2 [0.431]
^{103}Ru	39.35 days	3.043	6.948	497.1 [0.864], 610.3 [0.054]
^{95}Nb	34.97 days	6.496	4.893	765.8 [0.9982]
Activation Product				
^{60}Co	5.27 yr			1173.2 [1.00], 1332.5 [1.00]
^{58}Co	70.3 days			811.1 [0.99], 511.0[c]
^{54}Mn	312.2 days			834.8 [1.00]

[a]Europium-154 and ^{134}Cs values are given only for direct production of the isotope from the fission process. Each isotope is produced primarily through neutron absorption. For PWR fuel material irradiated to 25 GWd/tU, the "accumulated fission yields" of ^{154}Eu and ^{134}Cs were calculated as 0.15 and 0.46% for the total fissions, respectively.

[b]2.69-6 should be read as 2.69×10^{-6}.

[c]β^+ annihilation gamma ray.

C. Variability in Source Strength at One Axial Location

The measured gross gamma-ray doses varied by as much as 30% for the side measurements and 22% for the corner measurements (Tables XVI and XVII). Fuel assemblies C-52, C-70, and C-72 have the largest variabilities. The direction of the changes from one side or corner to the next is the same as it was for the neutron results; however, the relative magnitudes of the changes for the neutron and gamma-ray data are different. The neutron results vary as a power function of the exposure, and the gamma-ray results should vary as a linear function of exposure if one were to ignore the effects of the various half-lives of the gamma-emitting isotopes. Thus, the calculated exposure for the neutron case is less sensitive to the counting rate variations. For example, a 10% change in the neutron rate represents only a 3% change in the exposure, whereas a 10% change in the gamma-ray rate represents a 10% change in the calculated exposure. Figures 20 and 21 show the two sets of data plotted as a function of measurement position.

TABLE XVI

MEASURED GAMMA-RAY RESULTS FOR THE SQUARE-RING DETECTOR

Fuel Assembly	Declared Exposure (GWd/tU)	Cooling Time (Days)	Measured Gamma-Ray Dose				
			Side 1	Side 2	Side 3	Side 4	Total
A-72	18.47	2445	408	390	457	442	1697
A-54	20.81	2445	523	492	525	518	2058
A-74	20.84	2445	516	548	538	465	2067
A-73	20.91	2445	585	513	469	490	2057
D-31	23.43	2049	618	720	748	581	2667
C-32	23.57	2638	585	406	434	572	1997
D-26	26.91	2049	682	809	872	783	3146
C-51	28.90	1947	776	956	924	857	3513
B-52	31.71	1947	1102	1000	1026	1015	4143
C-52	32.82	1575	1610	1166	1017	1273	5066
C-70	33.08	1575	1109	1156	1560	1276	5101
C-72	37.85	1575	1684	1391	1461	1579	6115
C-56	40.07	1575	1599	1562	1692	1556	6409
C-64	40.55	1575	1747	1620	1572	1525	6464

TABLE XVII

MEASURED GAMMA-RAY RESULTS FOR THE CORNER V-DETECTOR

Fuel Assembly	Declared Exposure (GWd/tU)	Cooling Time (Days)	Measured Gamma-Ray Dose				
			Corner A	Corner B	Corner C	Corner D	Total
A-72	18.47	2445	214	188	202	224	828
A-54	20.81	2445	247	256	258	245	1006
A-74	20.84	2445	253	248	249	252	1002
A-73	20.91	2445	240	240	216	215	911
D-31	23.43	2049	334	378	312	268	1292
C-32	23.57	2638	257	186	216	289	948
D-26	26.91	2049	418	395	330	361	1504
C-51	28.90	1947	491	443	336	398	1577
B-52	31.71	1947	528	508	486	501	2023
C-52	32.82	1575	513	483	681	684	2361
C-70	33.08	1575	710	670	488	584	2452
C-72	37.85	1575	813	684	684	806	2984
C-56	40.07	1575	795	810	774	727	3106
C-64	40.55	1575	812	800	773	738	3123

D. Axial Gross Gamma-Ray Profiles

The axial gross gamma-ray profiles were measured for the same four fuel assemblies shown in Fig. 17 to demonstrate the relative flat response on the central regions of the fuel assemblies. Figure 22 shows the results for each of the four sides of the fuel assemblies. The variability between the measurements of each side is less than was noted in Fig. 17 for the neutron measurements because the gamma-ray dose is directly related to the exposure and cooling times, whereas the neutron signal is related to exposure by a power function.

E. Correlation Between Declared Cooling Times and Measured Doses

The internal consistency of a set of similar fuel assemblies can be verified by calculating the correlation between the measured gamma-ray doses divided by the declared exposure vs the declared cooling times of the fuel

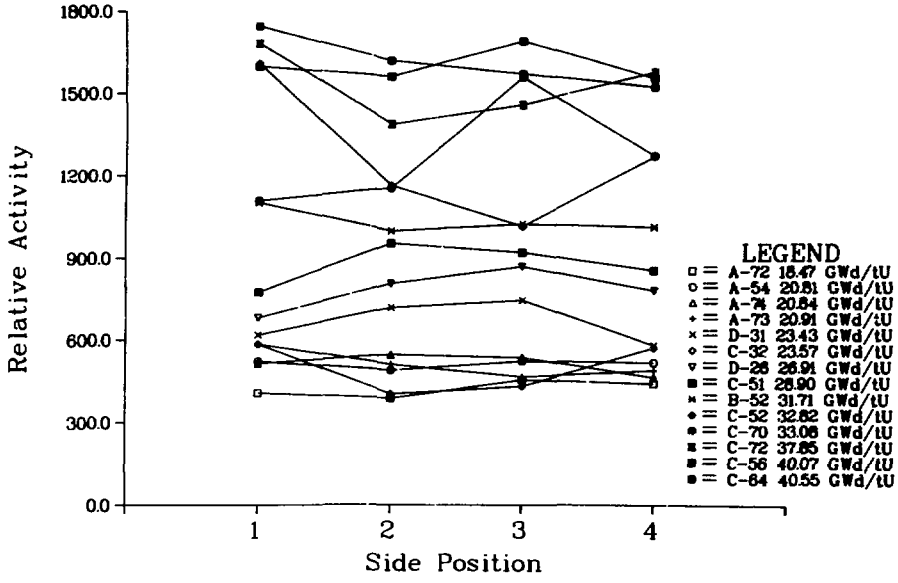

Fig. 20. Measured gross gamma-ray dose rates for each side of the 14 irradiated fuel assemblies.

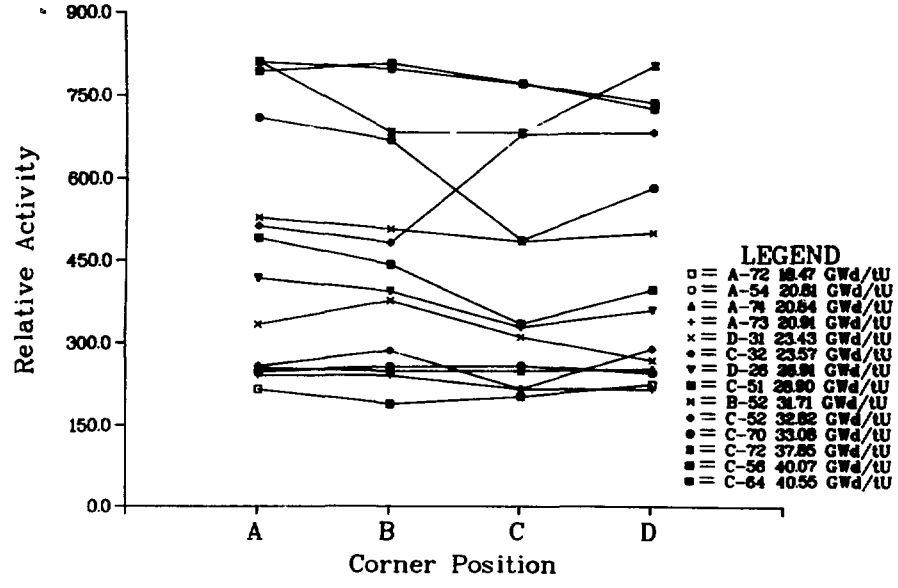

Fig. 21. Measured gross gamma-ray dose rates for each corner of the 14 irradiated fuel assemblies.

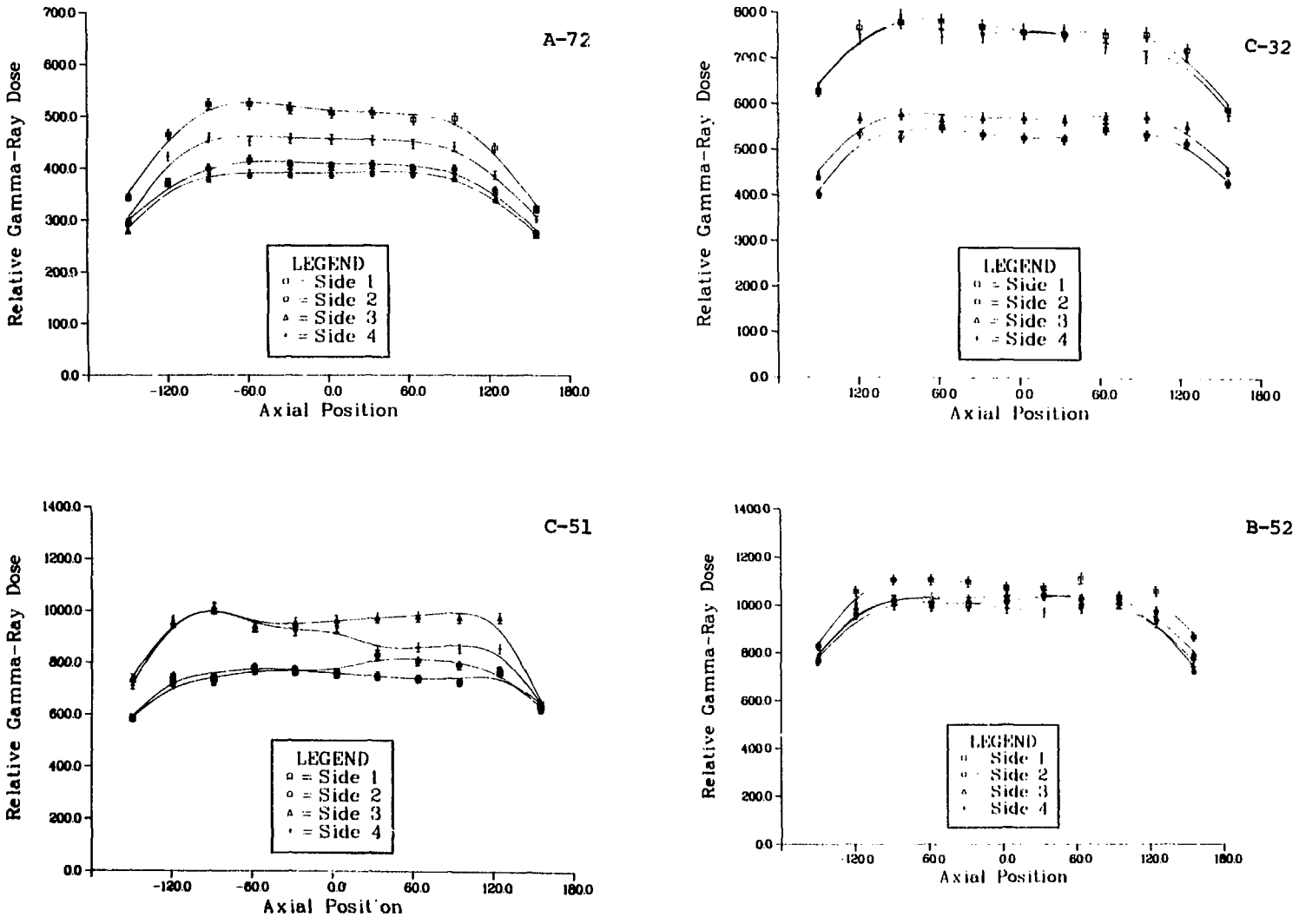

Fig. 22. **Axial gross gamma-ray profile for each side of the four fuel assemblies: A-72 (18.47 GWd/tU), C-32 (23.57 GWd/tU), C-51 (28.91 GWd/tU), and B-52 (31.71 GWd/tU).**

assemblies. Figures 23 and 24 show the results for the side and corner measurements, respectively. Table XVIII gives the data plotted in Figs. 23 and 24. Table XIX shows the computed results using the least squares fitted line in Figs. 23 and 24, in which the side measurements give an average difference of 2.3% and the corner measurements give an average difference of 3.3%. We stress that these measurements are only a check of the internal consistency of a specific set of fuel assemblies. The number of days of cooling could be changed by a constant factor, and this analysis would not show any differences between the altered cooling times and the measured dose divided by the declared exposure values.

This analysis also assumes that the irradiation histories of the fuel assemblies are very similar because of the short half-lives of all the fission products except for ^{137}Cs ($t_{1/2}$ = 30.17 yr). If a fuel assembly had an irregular irradiation history (for example, if it had been in the core for two cycles and out for two cycles followed by one more cycle in the core), its gamma dose as a function of cooling time would be significantly different from a fuel assembly in for three consecutive cycles. The contributions from ^{144}Ce-Pr (284.5 days), ^{106}Ru-Rh (366.4 days), and ^{134}Cs (2.062 yr) for the first two cycles would be much lower for the fuel assembly with the irregular irradiation history than for the fuel assembly with the constant irradiation history.

F. Position Sensitivity for the Square-Ring Detector

The sensitivity of the gross gamma-ray measurements to the relative positions of a fuel assembly within the square-ring detector was determined by positioning the B-52 fuel assembly at 11 different locations and measuring the outputs of the four ion chambers (Table XX). The total dose measurements varied by an average of less than 1% (0.6%) for the set. Comparable variations in the neutron measurements were 3.7%. However, the effect on the burnup results is similar (~1%) because of the neutron power functional relationship relative to the exposure. Because the gross gamma-ray signal is attenuated much less than is the neutron signal for the same thickness of water, positioning is less critical for these measurements.

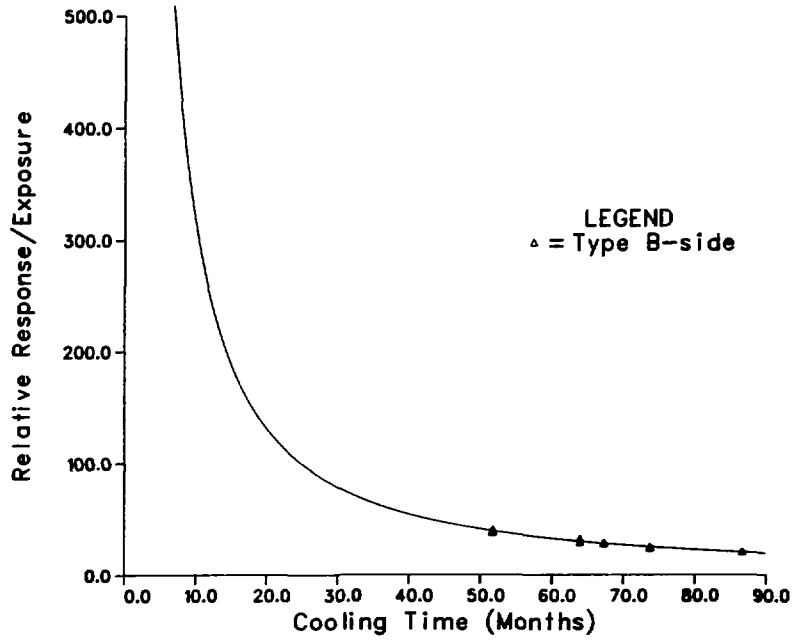

Fig. 23. Gross gamma-ray dose/exposures vs cooling time for the set of 14 fuel assemblies using the square-ring detector. (Refer to Fig. 3 for calculated response.)

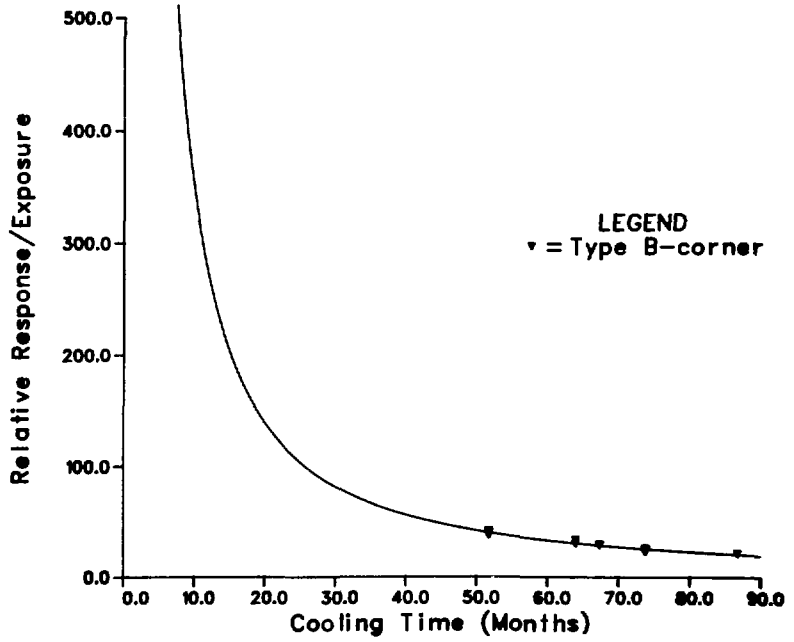

Fig. 24. Gross gamma-ray dose/exposure vs cooling time for the set of 14 fuel assemblies using the corner V-detector. (Refer to Fig. 3 for calculated response.)

TABLE XVIII

RELATIVE GAMMA-RAY MEASUREMENTS OF FUEL ASSEMBLIES

Fuel Assembly	Declared Exposure (GWd/tU)	Declared Cooling Time (Days)	Measured Dose[a] Side	Measured Dose[a] Corner	Dose/Exposure Side	Dose/Exposure Corner
A-72	18.47	2445	1697	828	91.9	44.8
A-54	20.81	2445	2058	1006	98.9	48.3
A-74	20.84	2445	2067	1002	99.2	48.1
A-73	20.91	2445	2057	911	98.4	43.6
D-31	23.43	2049	2667	1292	113.8	55.1
C-32	23.57	2638	1997	948	84.7	40.2
D-26	26.91	2049	3146	1504	116.9	55.9
C-51	28.90	1947	3513	1577	121.9	54.6
B-52	31.71	1947	4143	2023	130.7	63.8
C-52	32.82	1575	5066	2361	154.4	71.9
C-70	33.08	1575	5101	2452	154.2	74.1
C-72	37.85	1575	6115	2984	161.6	78.8
C-56	40.07	1575	6409	3106	159.9	77.5
C-64	40.55	1575	6464	3123	159.4	77.0

[a]Relative units for all four sides or corners.

VI. CONCLUSIONS AND RECOMMENDATIONS

This report concentrated on the evaluation of nondestructive techniques used to verify rapidly the operator-declared values for exposures and to verify the consistency of the declared cooling times. We evaluated using gross gamma-ray and neutron measurement techniques to provide the inspector with the capability to verify spent-fuel assemblies. These accurate and timely measurements can be performed with minimal interference to the facility operator. The value of such measurements should be considered in the context of the entire inspection process. For example, these techniques can be used with item counting or Cerenkov light measurements to improve the level of verification presently available to the IAEA inspection.

TABLE XIX

RESULTS OF COOLING TIME CONSISTENCY CALCULATIONS

Fuel Assembly	Declared Cooling Time (Days)	Calculated Cooling Time			
		Side		Corner	
		Days	Difference (%)	Days	Difference (%)
A-72	2445	2538	3.8	2479	1.4
A-54	2445	2379	-2.7	2323	-5.0
A-74	2445	2373	-2.9	2332	-4.6
A-73	2445	2390	-2.3	2538	3.8
D-31	2049	2103	2.7	2074	1.2
C-32	2638	2726	-3.4	2722	-3.2
D-26	2049	2054	0.3	2048	0.0
C-51	1947	1980	1.7	2090	7.3
B-52	1947	1862	-4.3	1827	-6.2
C-52	1575	1609	2.1	1648	4.6
C-70	1575	1611	2.3	1606	1.9
C-72	1575	1546	-1.9	1523	-3.3
C-56	1575	1560	-0.9	1545	-1.9
C-64	1575	1564	-0.7	1553	-1.4
Average absolute difference (%)			2.3		3.3
Parameters[a]					
a		689061.		382341.	
b		-1.138		-1.158	
R^2		0.9831		0.9619	

Equation used to approximate dose rate/exposure vs cooling time

$$\frac{DR}{EXP} = a \times T^b$$

[a] R^2 is the correlation coefficient. When multiplied by 100, it represents the percentage of the total mean variation explained by the regression.

TABLE XX

POSITION SENSITIVITY FOR GROSS GAMMA-RAY MEASUREMENTS USING THE SQUARE-RING DETECTOR

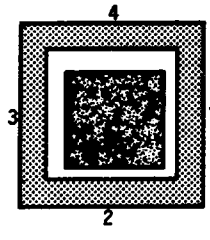

Side 1	52.5
Side 2	47.5
Side 3	46.3
Side 4	46.3
Total	192.6

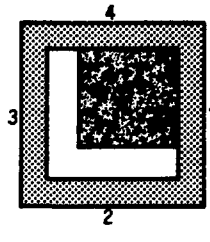

Side 1	61.9
Side 2	37.9
Side 3	39.4
Side 4	57.5
Total	196.3

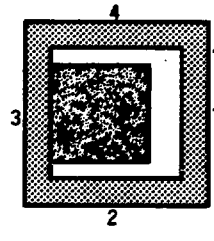

Side 1	41.6
Side 2	43.8
Side 3	61.3
Side 4	48.1
Total	193.8

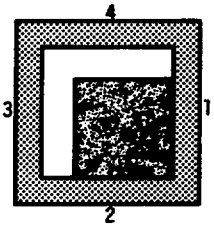

Side 1	61.3
Side 2	55.6
Side 3	38.7
Side 4	39.4
Total	195.1

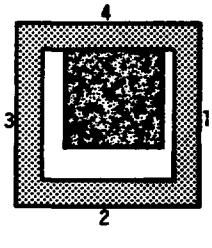

Side 1	52.5
Side 2	37.9
Side 3	46.6
Side 4	58.8
Total	195.8

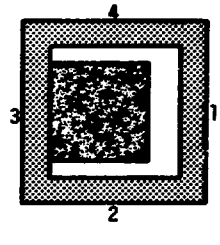

Side 1	48.1
Side 2	48.1
Side 3	52.5
Side 4	45.6
Total	194.3

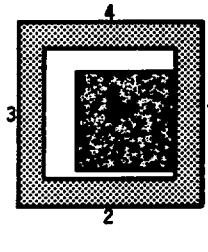

Side 1	62.5
Side 2	48.8
Side 3	39.4
Side 4	44.4
Total	195.1

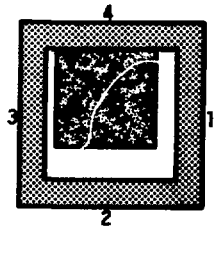

Side 1	41.3
Side 2	37.1
Side 3	58.8
Side 4	58.1
Total	195.2

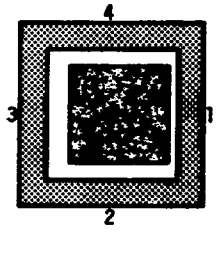

Side 1	61.1
Side 2	49.4
Side 3	41.6
Side 4	44.4
Total	194.4

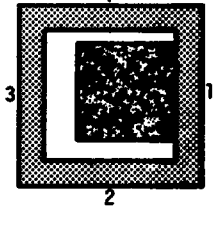

Side 1	62.5
Side 2	39.4
Side 3	39.4
Side 4	55.6
Total	195.1

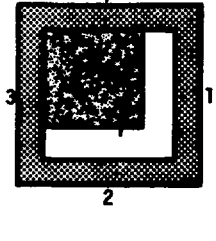

Side 1	41.1
Side 2	36.8
Side 3	61.3
Side 4	58.1
Total	196.2

Average total 194.9 ± 1.1 (1.6%)

[a]The results are relative numbers that are proportional to the current measured in the ionization chambers.

Passive neutron measurements can determine rapidly the relative exposures of irradiated fuel assemblies with an average absolute difference of approximately 4%, using the power functional relationship correlating exposure with the measured counting rates. Similar results are obtained if either the sides or corners of the fuel assemblies are measured. Using fission chambers horizontal to the principal axis of the fuel assembly may reduce the effects of burnup gradients across the fuel assembly, because vertical detectors measure fewer pins. Using either detector configuration, 1% counting statistics can be obtained within 10 to 30 s for fuel assemblies with 18.4- to 40.6-GWd/tU exposures and from 1575 to 2638 days of cooling.

Gross gamma-ray dose measurements can be used to determine rapidly the consistency of a set of declared cooling times by plotting the dose/exposure vs declared cooling times and inspecting the plot for data points that do not lie within the expected limits. This is a qualitative measurement; however, it is a convenient method for obtaining information about the declared cooling times.

Two detector designs that could be used by IAEA inspectors for the rapid verification of spent-fuel assemblies are shown in Fig. 25. One design consists of a single set of detectors that would measure the signals emanating from only one side of the fuel assembly. The other design contains two sets of detectors placed horizontally on opposite sides of the fuel assembly. This detector arrangement would partly compensate for exposure gradients across the fuel assembly, as gradients of 20 to 30% have been measured in this investigation. As discussed in Sec. IV.C.5, two detectors placed on opposite sides of the fuel assembly would give slightly better results than just one set of detectors. However, the improvement would only be about 1%, with both detector designs providing results in the 5% range.

Both the neutron and gross gamma-ray measurements can be obtained rapidly using either detector design described and the ION-1 electronics unit. To perform the measurements, the fuel assemblies must be raised until the top half of the assembly is out of the storage racks at the bottom of the pool. Measuring these two signatures gives a significantly higher level of verification of the inspection than does item counting or Cerenkov light measurements. Again we stress that any inspection procedure must consist of a combination of containment/surveillance accounting and measurement technique to provide an acceptable level of verification within the manpower and time restrictions.

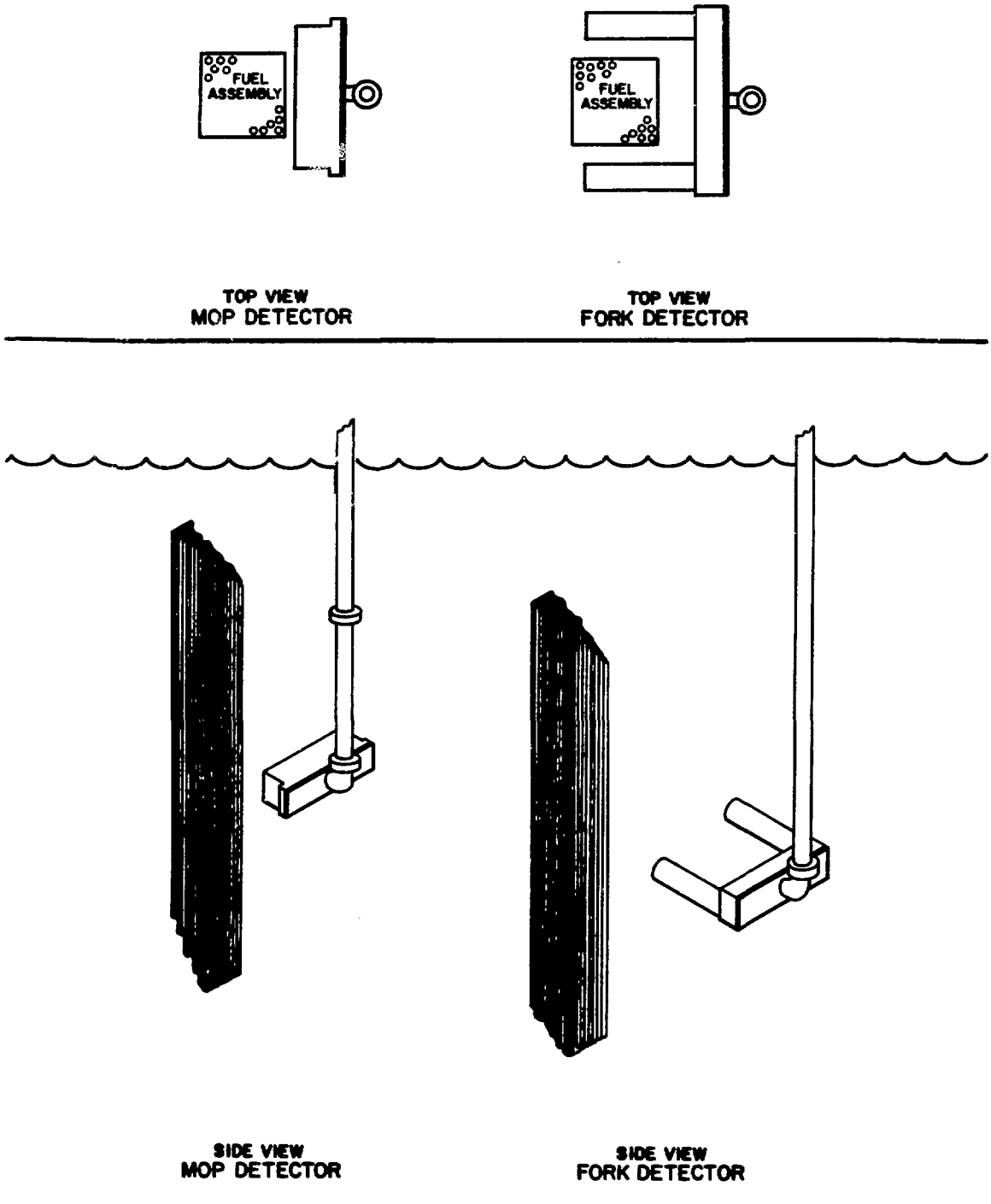

Fig. 25. Two detector designs for the rapid verification of spent-fuel assemblies.

ACKNOWLEDGMENTS

We extend our gratitude to F. A. Duran and O. R. Holbrooks for their support throughout the measurement exercise. We also appreciate the assistance of P. M. Rinard in preparing the curves relating the gamma dose rate to the declared exposure and cooling time values. General Electric personnel at the Morris operation Spent-Fuel Storage Facility provided expert assistance during the measurements. We also gratefully acknowledge the support of the International Safeguards Office at Brookhaven National Laboratory and the DOE Office of Safeguards and Security.

REFERENCES

1. "Non-Proliferation and International Safeguards," International Atomic Energy Agency report IAEA-575 (1978).

2. "The Structure and Content of Agreements between the Agency and States Required in Connection with the Treaty on the Non-Proliferation of Nuclear *Weapons*," International Atomic Energy Agency report INFCIRC/153 (corrected) (June 1971).

3. H. Gruemm, "Designing IAEA Safeguards Approaches," Nucl. Mater. Manage. IX, 14-24 (July 1980).

4. "IAEA Contribution to INFCE--The Present Status of IAEA Safeguards on Nuclear Fuel Cycle Facilities," International Atomic Energy Agency report INFCE/SEC/11 (February 1979).

5. "IAEA Safeguards Technical Manual, Introduction, Part A," International Atomic Energy Agency report IAEA-174 (1976).

6. D. D. Cobb, H. A. Dayem, and R. J. Dietz, "Preliminary Concepts: Safeguards for Spent Light-Water Reactor Fuels," Los Alamos Scientific Laboratory report LA-7730-MS (June 1979).

7. "Advisory Group Meeting on Methods and Techniques for NDA Safeguards Measurements of Power Reactor Spent Fuel," International Atomic Energy Agency report AG-241, Vienna, October 29-November 2, 1979.

8. E. J. Dowdy, N. Nicholson, and J. T. Caldwell, "Irradiated Fuel Monitoring by Cerenkov Glow Intensity Measurements," Los Alamos Scientific Laboratory report LA-7838-MS (ISPO-61) (September 1979).

9. N. Nicholson and E. J. Dowdy, "Irradiated Fuel Examination Using the Cerenkov Technique," Los Alamos National Laboratory report LA-8767-MS (March 1981).

10. C. E. Moss and D. M. Lee, "Gross Gamma-Ray Measurements of Light Water Reactor Spent-Fuel Assemblies in Underwater Storage Arrays," Los Alamos Scientific Laboratory report LA-8447 (ISPO-132) (December 1980).

11. D. M. Lee, J. R. Phillips, S.-T. Hsue, K. Kaieda, J. K. Halbig, E. G. Medina, and C. R. Hatcher, "A New Approach to the Examination of LWR Irradiated Fuel Assemblies Using Simple Gas Chamber Techniques," Los Alamos Scientific Laboratory report LA-7655-MS (ISPO-48) (March 1979).

12. P. M. Rinard, "Irradiated Fuel Inspection in a Storage Pond with No Fuel Movement and an Uncollimated Detector," Los Alamos Scientific Laboratory report LA-8463-MS (ISPO-110) (July 1980).

13. S. T. Hsue, J. E. Stewart, K. Kaieda, J. K. Halbig, J. R. Phillips, D. M. Lee, and C. R. Hatcher, "Passive Neutron Assay of Irradiated Nuclear Fuels," Los Alamos Scientific Laboratory report LA-7645-MS (February 1979).

14. J. R. Phillips, G. E. Bosler, J. K. Halbig, S. F. Klosterbuer, D. M. Lee, and H. O. Menlove, "Neutron Measurement Techniques for the Nondestructive Analysis of Irradiated Fuel Assemblies," Los Alamos National Laboratory report LA-9002-MS (ISPO-156) (November 1981).

15. T. N. Dragnev, "Intrinsic Self-Calibration of Non-Destructive Gamma Spectrometric Measurements (Determination of U, Pu, and Am-241 Isotopic Ratios)," International Atomic Energy Agency report IAEA/STR-60 (Vienna 1976).

16. J. R. Phillips, J. K. Halbig, D. M. Lee, S. E. Beach, T. R. Bement, E. Dermendjiev, C. R. Hatcher, K. Kaieda, and E. G. Medina, "Application of Nondestructive Gamma-Ray and Neutron Techniques for the Safeguarding of Irradiated Fuel Materials," Los Alamos Scientific Laboratory report LA-8212 (ISPO-77) (May 1980).

17. S. T. Hsue, C. R. Hatcher, and K. Kaieda, "Cooling Time Determination of Spent Fuel," Nucl. Mater. Manage. VIII, 356-367 (fall 1979).

18. J. K. Halbig and S. F. Klosterbuer, "Portable Spent-Fuel Gamma-Ray and Neutron Detector Electronics User Manual," to be published as LA-8707-M.

19. P. I. Fedotov, N. M. Kazarinov, and A. A. Voronkov, "The Use of Neutron Scanning Method for Analysis of Spent VVER Fuel in Safeguarding System," Proc. 3rd Ann. ESARDA Symp. Safeguards Nucl. Mater. Manage., Karlsruhe, Federal Republic of Germany, 1981.

20. D. D. Cobb, J. R. Phillips, G. E. Bosler, G. W. Eccleston, J. K. Halbig, C. R. Hatcher, and S-T. Hsue, "Nondestructive Verification and Assay Systems for Spent Fuels," Los Alamos National Laboratory report LA-9041 Vol. 1 (April 1982).

★ U.S. GOVERNMENT PRINTING OFFICE: 1982-0-676-026/168